

# The form factors of $\tau \rightarrow K\pi(\eta)\nu$ and the predictions for CP violation beyond the standard model

D. Kimura,<sup>1</sup> Kang Young Lee<sup>2</sup> and T. Morozumi<sup>3</sup>

<sup>1</sup>*Faculty of Education, Hiroshima University,*

*Higashi-Hiroshima, 739-8524, Japan*

<sup>2</sup>*Division of Quantum Phases and Devices,*

*School of Physics, Konkuk University, Seoul, 143-701, Korea*

<sup>3</sup>*Graduate School of Science, Hiroshima University,*

*Higashi-Hiroshima, 739-8526, Japan*

## Abstract

We study the hadronic form factors of  $\tau$  lepton decays  $\tau \rightarrow K\pi(\eta)\nu$ . We compute one loop corrections to the form factors using the chiral Lagrangian including vector mesons. In the vector form factor,  $K^*$  resonance behavior is reproduced by resumming the vector meson self-energy diagrams. We fit the data of the hadronic invariant mass spectrum measured by Belle by determining some of the counterterms of the Lagrangian. Besides the hadronic invariant mass spectrum, the forward and backward asymmetry is predicted. We also study the effect of CP violation of a two Higgs doublet model. In the model, CP violation of the neutral Higgs sector generates the mixing of CP even Higgs and CP odd Higgs. We show how the mixing leads to the direct CP violation of the  $\tau$  decays and predict the CP violation of the forward and backward asymmetry.

## I. INTRODUCTION

The tau hadronic decays are unique as the decays can be useful for the search for the new CP violation beyond the standard model [1–12]. CP violation in tau lepton semileptonic decays has been searched in  $\tau \rightarrow \pi\pi\nu$  [13] and  $\tau \rightarrow K\pi\nu$  [14, 15] modes. Recently, Belle [15] puts constraint on the CP violation parameter of three Higgs doublet model with their latest data. In  $\tau$  lepton system, another CP violating observable, e.d.m. (electric dipole moment) is also searched [16].

To predict the direct CP violation of the hadronic  $\tau$  decays, the strong phase shifts are important quantities and the quantitative prediction on the strong phase shifts is necessary when extracting the weak CP violating phases from the experimentally observed CP asymmetries [6, 10, 11]. This is a reason why we study the hadronic form factors.

The hadronic form factors for the decay  $\tau \rightarrow K\pi\nu$  have been studied with various methods. The common future of them is the effects of  $K^*(892)$  meson and higher resonances are included. In Ref.[5, 17], vector dominance models are studied. Resonance chiral perturbation theory with the dispersion relations are used in Ref. [18–21]. In our previous study, we use the resonance chiral Lagrangian including the one loop corrections to the self-energy of resonance [10]. We also note in the experimental study [22], the Breit Wigner form for several resonances is used to fit the data of the hadronic invariant mass spectrum.

In this paper, we use different approach from the previous study [10]. By using the chiral Lagrangian including vector resonance [23], we resum the self-energy corrections to the vector mesons. By resumming them one can reproduce the resonance behavior near the poles of the resonances while keeping prediction at threshold region consistent with the chiral perturbation theory. Our Lagrangian includes several new counterterms related to vector mesons. Since Belle and Babar reported the precise measurements of the branching fractions of  $\tau^- \rightarrow K_s\pi^-\nu$  [22],  $\tau^- \rightarrow K^-\pi^0\nu$  [25] and  $\tau^- \rightarrow K^-\eta\nu$  [26, 27], we can compare our prediction of the hadronic invariant mass distribution with the experimental data. We have determined some of the counterterms so that the hadronic invariant mass spectrum is reproduced.

Once the form factors are fixed, one can use them for predictions of various distributions within the standard model and beyond. We first compute the angular distribution and the forward and backward asymmetry(FBA) for  $\tau \rightarrow K\pi\nu$  and  $\tau \rightarrow K\eta\nu$  in standard model [28].

Furthermore, CP violation of FBA is predicted with a two Higgs doublet model. In type II two Higgs doublet model, within the tree level approximation, the charged Higgs couplings with quarks and leptons are written in terms of CKM(Cabibbo-Kobayashi-Maskawa) matrix. However, if we take into account the one loop corrections to the masses of quarks and leptons due to the neutral Higgs exchanged diagrams, CP violation of the neutral Higgs sector becomes a new source of CP violation of the charged Higgs Yukawa couplings. We show the CP violation of the type II two Higgs doublet model can be probed by the direct CP violation of the  $\tau$  hadronic decays.

The paper is organized as follows. In section II, we show the hadronic chiral Lagrangian with the vector resonances which are relevant for the form factors. The counterterms are also given. In section III, we compute the form factors by showing how to resum the self-energy corrections. In section IV, we calculate the hadronic invariant mass spectra of the decays  $\tau \rightarrow K\pi(\eta)\nu$ . The spectra are compared with the experimental data and the FBAs are predicted. In section V, we explain how CP violation in neutral Higgs sector reveals itself in the charged Higgs Yukawa couplings in a two Higgs doublet model (2HDM). We also calculate the CP violation of FBA of the hadronic  $\tau$  decays and the numerical result is presented. Section VI is devoted to discussion and summary. In appendix, we give some details of the derivation of the formulae used in the text.

## II. CHIRAL LAGRANGIAN WITH VECTOR MESONS

The leading order  $O(p^2)$  of chiral Lagrangian with  $\eta_0 - \eta_8$  mixing term and vector meson mass term is given by,

$$\begin{aligned} \mathcal{L} = & \frac{f^2}{4}\text{Tr}(D_L U D_L U^\dagger) + B\text{Tr}[M(U + U^\dagger)] - ig_{2p}\text{Tr}(\xi M \xi - \xi^\dagger M \xi^\dagger) \cdot \eta_0 - \frac{M_0^2}{2}\eta_0^2 \\ & + M_V^2 \text{Tr} \left[ \left( V_\mu - \frac{\alpha_\mu}{g} \right)^2 \right], \end{aligned} \quad (1)$$

where  $U$  is the chiral field which is given as  $U = \exp(2i\pi/f) = \xi^2$ .  $\pi$  is SU(3) octet pseudoscalar and  $B$  is a constant parameter.  $\eta_0$  is U(1)<sub>A</sub> pseudoscalar of which mass is denoted by  $M_0$  and  $g_{2p}$  is the coupling for  $\eta_0 - \eta_8$  mixing. The covariant derivative for the chiral field  $U$  is given by,

$$D_{L\mu}U = (\partial_\mu + iA_{L\mu})U, \quad (2)$$

where the external gauge field of  $SU(3)_L$  denoted by  $A_L$  is introduced.  $V_\mu$  is the vector nonets and  $\alpha_\mu$  is defined as,

$$\begin{aligned}\alpha_\mu &= \frac{\xi^\dagger D_{L\mu} \xi + \xi \partial_\mu \xi^\dagger}{2i} \\ &= \alpha_\mu^0 + \frac{\xi^\dagger A_{L\mu} \xi}{2}.\end{aligned}\quad (3)$$

The form of the Lagrangian at leading order is identical to the one of the unitary gauge fixed version of hidden local symmetry approach [23, 24]. Note that we have added the chiral breaking term by  $M = \text{diag}(m_u, m_d, m_s)$  for the pseudoscalar mesons.

In the Lagrangian, there is no kinetic term for the vector meson at the leading order. The kinetic term is generated as the loop correction of the pseudoscalar mesons. In chiral counting, the vector meson fields  $V_\mu$  are counted as is  $O(p)$  and the chiral breaking  $\chi$  is counted as  $O(p^2)$ . The counterterms at  $O(p^4)$  are given as,

$$\begin{aligned}\mathcal{L}_c &= -\frac{1}{2} Z_V \text{Tr}(F_{V\mu\nu} F_V^{\mu\nu}) \\ &+ C_1 \text{Tr} \left[ \frac{\xi \chi \xi + \xi^\dagger \chi^\dagger \xi^\dagger}{2} \left( V_\mu - \frac{\alpha_\mu}{g} \right)^2 \right] + C_2 \text{Tr} \left( \frac{\xi \chi \xi + \xi^\dagger \chi^\dagger \xi^\dagger}{2} \right) \text{Tr} \left[ \left( V_\mu - \frac{\alpha_\mu}{g} \right)^2 \right] \\ &+ i C_3 \text{Tr}(F_V^{\mu\nu} \alpha_{\perp\mu} \alpha_{\perp\nu}) + C_4 \text{Tr}(\xi F_V^{\mu\nu} \xi^\dagger F_{L\mu\nu}) + \mathcal{L}_2,\end{aligned}\quad (4)$$

where  $F_{V\mu\nu} = \partial_\mu V_\nu - \partial_\nu V_\mu + ig[V_\mu, V_\nu]$  and  $F_{L\mu\nu} = \partial_\mu A_{L\nu} - \partial_\nu A_{L\mu}$ .  $Z_V$  and  $C_i$  ( $i = 1, \dots, 4$ ) are renormalization constants.  $z_V$  and  $c_i$  are the finite parts of them.  $\mathcal{L}_2$  is the  $O(p^4)$  counterterm of the chiral perturbation theory [29]. The chiral breaking term  $\chi$  in the isospin limit can be written by the masses of  $\pi$  and  $K$  mesons as,

$$\begin{aligned}\chi &= \frac{4BM}{f^2} \\ &= \begin{pmatrix} m_\pi^2 & 0 & 0 \\ 0 & m_\pi^2 & 0 \\ 0 & 0 & 2m_K^2 - m_\pi^2 \end{pmatrix}.\end{aligned}\quad (5)$$

$\alpha_\perp$  in Eq.(4) is given as,

$$\alpha_{\perp\mu} = \frac{\xi^\dagger D_{L\mu} \xi - \xi \partial_\mu \xi^\dagger}{2i}.\quad (6)$$

By setting the external field  $A_L$  zero and expanding  $e^{i\frac{\pi}{f}}$  in  $\alpha$  and  $\alpha_\perp$ , we obtain the leading

terms of the expansion as,

$$\begin{aligned}\alpha_\mu &= \frac{[\pi, \partial_\mu \pi]}{2if^2}, \\ \alpha_{\perp\mu} &= \frac{\xi^\dagger \partial_\mu U \xi^\dagger}{2i} = \frac{\partial_\mu \pi}{f}.\end{aligned}\quad (7)$$

The mass matrix for  $\eta_0$  and  $\eta_8$  sector is extracted from Eq.(1),

$$\mathcal{L}_{08} = -\frac{1}{2}(\eta_8, \eta_0) \begin{pmatrix} M_{88}^2 & M_{08}^2 \\ M_{08}^2 & M_{00}^2 \end{pmatrix} \begin{pmatrix} \eta_8 \\ \eta_0 \end{pmatrix} = -\frac{1}{2}(\eta, \eta') \begin{pmatrix} m_\eta^2 & 0 \\ 0 & m_{\eta'}^2 \end{pmatrix} \begin{pmatrix} \eta \\ \eta' \end{pmatrix}, \quad (8)$$

with,

$$\begin{pmatrix} \eta \\ \eta' \end{pmatrix} = \begin{pmatrix} \cos \theta_{08} & -\sin \theta_{08} \\ \sin \theta_{08} & \cos \theta_{08} \end{pmatrix} \begin{pmatrix} \eta_8 \\ \eta_0 \end{pmatrix}, \quad (9)$$

where  $M_{88}^2 = (4m_K^2 - m_\pi^2)/3$ . From Eq.(8),  $M_{00}$  and  $M_{08}$  are written by,

$$M_{00}^2 = m_\eta^2 + m_{\eta'}^2 - M_{88}^2, \quad (10)$$

$$M_{08}^2 = -\sqrt{M_{00}^2 M_{88}^2 - m_\eta^2 m_{\eta'}^2}. \quad (11)$$

The mixing angle  $\theta_{08}$  is given by,

$$\theta_{08} = -\frac{1}{2} \arctan \frac{2|M_{08}^2|}{M_{00}^2 - M_{88}^2}. \quad (12)$$

### III. THE FORM FACTORS AT $O(p^4)$

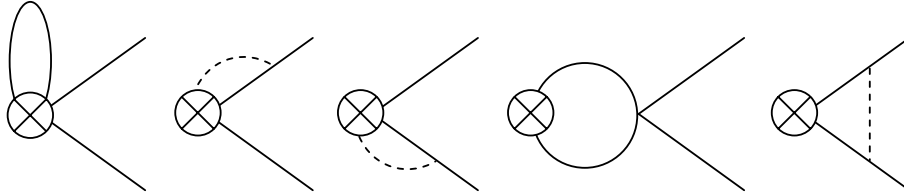


FIG. 1: 1 particle irreducible and one loop Feynman diagrams which contribute to the  $W^+ \rightarrow K^+ \pi^0$  vertex. The crossed circle denotes the weak vertex. The solid lines correspond to the pseudoscalar bosons and the dashed lines correspond to the vector bosons.

In this section, we compute the form factors. The matrix elements of the current  $\bar{u}\gamma_\mu s$  are obtained by identifying the quark current with the corresponding current of the chiral

Lagrangian, Eq.(1) and Eq.(4). If we compute the form factor within rigorous one loop approximation, we must use  $\frac{1}{M_V^2}$  as the vector meson propagator since there is no kinetic term for vector meson in the lowest order Lagrangian. In the one loop calculation, we can show that the form factors calculated with such propagator, are identical to those obtained with chiral perturbation theory [11]. In  $\tau \rightarrow K\pi\nu$  process,  $K^*$  meson which produced by the strangeness changing current can contribute to the vector form factor. The resonant contribution is significant when  $K\pi$  invariant mass is near to the resonance pole. In this region, momentum expansion is not valid. Therefore we need to go beyond the chiral perturbation. We take into account the resonance by using the Dyson summed propagator. Instead of using the tree level propagator with the form proportional to  $\frac{1}{M_V^2}$ , we use the resummed propagator (Fig. 4). Since the propagator have a pole in complex plane, the effect of the width of resonance is included. Thus we can reproduce the resonance behavior. As we show below in detail, one may include the effect of resonance so that it does not change the result of chiral perturbation theory near the threshold energy region for final hadrons.

In one loop diagrams, there are three categories of the diagrams. The first one is 1 particle irreducible (1PI) diagrams and are shown in Fig.1. They correspond to the one loop corrections to  $W^+ \rightarrow K^+\pi^0$  vertex. They include all the diagrams which are also present in chiral perturbation within one loop. Their contributions to the matrix element  $\langle K^+\pi^0 | \bar{u}_L \gamma_\mu s_L | 0 \rangle$  become,

$$\begin{aligned}
& \langle K^+\pi^0 | \bar{u}_L \gamma_\mu s_L | 0 \rangle \Big|_{1\text{PI}} = \\
& -\frac{1}{24\sqrt{2}f^2} \left( 1 - \frac{M_V^2}{8g^2f^2} \right) [Q_\mu(3I_{\eta_8} + 2I_K - 5I_\pi) + q_\mu(3I_{\eta_8} + 7I_K + 5I_\pi)] \\
& + \frac{1}{24\sqrt{2}f^2} \left( 1 - \frac{M_V^2}{2g^2f^2} \right) \left[ \sum_{PQ} C_{PQ} I_\mu^{QP} + 2(\Sigma_{K\pi} \chi_\mu^{\pi K} - \Delta_{K\pi} \chi_\mu^{\eta_8 K}) + 3(J_\mu^{\pi K} + J_\mu^{\eta_8 K}) \right] \\
& + \frac{M_V^2}{32\sqrt{2}g^2f^4} [q_\mu(3I_{\eta_8} + 6I_K + 3I_\pi) - 3(J_\mu^{\pi K} + J_\mu^{\eta_8 K})] \\
& + \frac{M_V^4}{32\sqrt{2}g^4f^6} \frac{3}{2} (J_\mu^{\pi K} + J_\mu^{\eta_8 K}) + \frac{(2m_K^2 + m_\pi^2)C_2 + m_K^2 C_1}{4\sqrt{2}g^2f^2} q_\mu, \tag{13}
\end{aligned}$$

where  $Q = p_K + p_\pi$  and  $q = p_K - p_\pi$ .  $C_{PQS}$  are  $(C_{K\pi}, C_{K\eta_8}, C_{\pi K}) = (1, -3, -4)$ .  $\Delta_{PQ}$  denotes the mass squared difference  $\Delta_{PQ} = m_P^2 - m_Q^2$ .  $\Sigma_{PQ}$  denotes the sum of the mass squared  $\Sigma_{PQ} = m_P^2 + m_Q^2$ . The loop functions  $I_P, \chi_\mu^{QP}, J_\mu^{QP}, I_\mu^{QP}$ , are given in Eq.(A1) and Eq.(A2).

The diagrams in the second category are shown in Fig. 2. It includes the diagrams with a  $K^*$  propagator and one loop corrections to  $K^* \rightarrow K^+\pi^0$  vertex. If we use the propagator which is proportional to  $\frac{1}{M_V^2}$ , the contribution to the matrix element from the second category becomes,

$$\begin{aligned}
\langle K^+\pi^0 | \bar{u}_L \gamma_\mu s_L | 0 \rangle &= \frac{M_V^2}{48\sqrt{2}g^2f^4} \left[ \sum_{PQ} C_{PQ} I_\mu^{QP} + 2(\Sigma_{K\pi} \chi_\mu^{\pi K} - \Delta_{K\pi} \chi_\mu^{\eta_8 K}) + 3(J_\mu^{\pi K} + J_\mu^{\eta_8 K}) \right] \\
&\quad - \frac{M_V^2}{48\sqrt{2}g^2f^4} \left[ Q_\mu \frac{3I_{\eta_8} + 2I_K - 5I_\pi}{4} + q_\mu \frac{3I_{\eta_8} + 7I_K + 5I_\pi}{2} \right] \\
&\quad - \frac{M_V^4}{16\sqrt{2}g^4f^6} \frac{3}{4} (J_\mu^{\pi K} + J_\mu^{\eta_8 K}) - \frac{q_\mu}{4\sqrt{2}g^2f^2} [C_2(2m_K^2 + m_\pi^2) + C_1m_K^2] \\
&\quad - \frac{C_3}{8\sqrt{2}gf^2} (Q^2 q_\mu - \Delta_{K\pi} Q_\mu). \tag{14}
\end{aligned}$$

Now we derive the matrix element for which the resummed propagator for  $K^*$  meson (Eq.(16)) is used instead of using the propagator proportional to  $\frac{1}{M_V^2}$ . To obtain the result consistent with that of chiral perturbation, one should note that the sum of the first two lines in both Eq.(13) and Eq.(14) leads to the chiral perturbation result except for the counterterms. It implies that instead of replacing the propagator  $\frac{1}{M_V^2}$  with the resummed one in the whole amplitude in Eq.(14), one can replace it for the part of the amplitude, i.e., only for the third and the fourth lines in Eq.(14). If we replace it for the whole amplitude, one can not make the amplitude finite by choosing the coefficient of the counterterm  $C_3$ . Contrast to this, the divergence in the third line of Eq.(14) can be canceled by choosing the coefficient  $C_3$ , which also implies one should replace the propagator with the resummed one for the part of Eq.(14) as,

$$\begin{aligned}
& - \frac{M_V^4}{16\sqrt{2}g^4f^6} \frac{3}{4} (J_\mu^{\pi K} + J_\mu^{\eta_8 K}) - \frac{q_\mu}{4\sqrt{2}g^2f^2} [C_2(2m_K^2 + m_\pi^2) + C_1m_K^2] \\
& - \frac{C_3}{8\sqrt{2}gf^2} (Q^2 q_\mu - \Delta_{K\pi} Q_\mu) \\
\rightarrow & - \left\{ \frac{M_V^6}{16\sqrt{2}g^4f^6} \frac{3}{4} (J_{\rho\nu}^{\pi K} + J_{\rho\nu}^{\eta_8 K}) q^\nu + \frac{q_\rho M_V^2}{4\sqrt{2}g^2f^2} [C_2(2m_K^2 + m_\pi^2) + C_1m_K^2] \right. \\
& \left. + \frac{C_3 M_V^2}{8\sqrt{2}gf^2} (Q^2 g_{\nu\rho} - Q_\nu Q_\rho) q^\nu \right\} D_\mu^\rho \tag{15}
\end{aligned}$$

where the resummed propagator  $D_{\mu\rho}$  of  $K^*$  meson is given as,

$$D_{\mu\rho} = \frac{g_{\mu\rho} - \frac{Q_\mu Q_\rho \delta B}{M_V^2 + \delta A + Q^2 \delta B}}{M_V^2 + \delta A}. \tag{16}$$

where the self energy corrections  $\delta A$  and  $\delta B$  in this section are identical to the  $K^*$  mesons ones given in Eq.(B8),

$$\delta A = \delta A_{K^*}, \quad \delta B = \delta B_{K^*}. \quad (17)$$

After carrying out the replacement Eq.(15) in Eq.(14), one may sum the two contributions, which leads to the following contribution to the matrix element.

$$\begin{aligned} \langle K^+ \pi^0 | \bar{u}_L \gamma_\mu s_L | 0 \rangle = & -\frac{1}{24\sqrt{2}f^2} [Q_\mu(3I_{\eta_8} + 2I_K - 5I_\pi) + q_\mu(3I_{\eta_8} + 7I_K + 5I_\pi)] \\ & + \frac{1}{24\sqrt{2}f^2} \left[ \sum_{PQ} C_{PQ} I_\mu^{QP} + 2(\Sigma_{K\pi} \chi_\mu^{\pi K} - \Delta_{K\pi} \chi_\mu^{\eta_8 K}) + 3(J_\mu^{\pi K} + J_\mu^{\eta_8 K}) \right] \\ & + \frac{M_V^2}{32\sqrt{2}g^2 f^4} [q_\mu(3I_{\eta_8} + 6I_K + 3I_\pi) - 3(J_\mu^{\pi K} + J_\mu^{\eta_8 K})] \\ & + \frac{M_V^4}{32\sqrt{2}g^4 f^6} \frac{3}{2} (J_\mu^{\pi K} + J_\mu^{\eta_8 K}) + \frac{(2m_K^2 + m_\pi^2)C_2 + m_K^2 C_1}{4\sqrt{2}g^2 f^2} q_\mu \\ & - \left\{ \frac{M_V^6}{16\sqrt{2}g^4 f^6} \frac{3}{4} (J_{\rho\nu}^{\pi K} + J_{\rho\nu}^{\eta_8 K}) q^\nu + \frac{q_\rho M_V^2}{4\sqrt{2}g^2 f^2} [C_2(2m_K^2 + m_\pi^2) + C_1 m_K^2] \right. \\ & \left. + \frac{C_3 M_V^2}{8\sqrt{2}g f^2} (Q^2 g_{\nu\rho} - Q_\nu Q_\rho) q^\nu \right\} \frac{\delta_\mu^\rho - \frac{Q^\rho Q_\mu \delta B}{M_V^2 + \delta A + Q^2 \delta B}}{M_V^2 + \delta A} \\ & - \frac{q_\mu}{2\sqrt{2}} \left( \sqrt{Z_K Z_\pi} - 1 + 8L_4 \frac{2m_K^2 + m_\pi^2}{f^2} + 4L_5 \frac{\Sigma_{K\pi}}{f^2} \right) \\ & - \frac{1}{\sqrt{2}f^2} (Q^2 q_\mu - \Delta_{K\pi} Q_\mu) L_9 - \frac{4L_5}{2\sqrt{2}f^2} Q_\mu \Delta_{K\pi}, \quad (18) \end{aligned}$$

where we add the counterterms from the wave function renormalization denoted as  $Z_K$  and  $Z_\pi$  for the final states and  $O(p^4)$  counterterms corresponding to  $\mathcal{L}_2$  from chiral perturbation theory [29]. The latter contributions are proportional to the coefficients  $L_4$ ,  $L_5$  and  $L_9$  in Eq.(18).  $L_4$ ,  $L_5$  and wave function renormalizations are identical to those of the chiral

perturbation and we substitute them into Eq.(18). The result is,

$$\begin{aligned}
\text{Eq.(18)} = & \frac{1}{4\sqrt{2}g^2f^2} \left[ \left( q_\mu - \frac{\Delta_{K\pi}}{Q^2} Q_\mu \right) \frac{\delta A}{M_V^2 + \delta A} \left\{ \delta A + Q^2 \left( Z_V + \frac{gC_3}{2} \right) \right\} \right. \\
& + \left. \frac{\Delta_{K\pi}}{Q^2} Q_\mu \frac{(\delta A + Q^2 \delta B)^2}{M_V^2 + \delta A + Q^2 \delta B} \right] \\
& + \frac{3M_V^2}{8\sqrt{2}g^2f^2} \left[ \left( q_\mu - \frac{\Delta_{K\pi}}{Q^2} Q_\mu \right) (H_{K\pi}^0 + H_{K\eta_8}^0) - \frac{\Delta_{K\pi} Q_\mu}{Q^2 f^2} (L_{K\pi} + L_{K\eta_8}) \right] \\
& - \frac{1}{2\sqrt{2}} \frac{3}{2} (H_{K\pi}^0 + H_{K\eta_8}^0) \left( q_\mu - \frac{\Delta_{K\pi}}{Q^2} Q_\mu \right) - \frac{1}{2\sqrt{2}} \frac{\Delta_{K\pi}}{Q^2} Q_\mu \{ f_0(l_5^r, Q^2) - 1 \} \\
& - \frac{Q^2}{\sqrt{2}f^2} \left( q_\mu - \frac{\Delta_{K\pi} Q_\mu}{Q^2} \right) \left[ L_9 + \frac{C_3}{8g} \right. \\
& \left. + \frac{1}{128\pi^2} \left( 1 - \frac{M_V^2}{2g^2f^2} \right) (C_{UV} + 1 - \ln \mu^2) \right], \tag{19}
\end{aligned}$$

where  $f_0(l_5^r, Q^2)$  is identical to the scalar form factor in chiral perturbation theory which is shown in Eq.(2.6) of [30] and is given by,

$$\begin{aligned}
f_0(l_5^r, Q^2) = & 1 + \frac{1}{8f^2} \left( 5Q^2 - 2\Sigma_{K\pi} - 3\frac{\Delta_{K\pi}^2}{Q^2} \right) \bar{J}_{K\pi}(Q^2) \\
& + \frac{1}{24f^2} \left( 3Q^2 - 2\Sigma_{K\pi} - \frac{\Delta_{K\pi}^2}{Q^2} \right) \bar{J}_{K\eta_8}(Q^2) \\
& + \frac{Q^2}{4\Delta_{K\pi}} (5\mu_\pi - 2\mu_K - 3\mu_{\eta_8}) + 4\frac{l_5^r}{f^2} Q^2, \tag{20}
\end{aligned}$$

where  $\mu_P = \frac{M_P^2}{32\pi^2 f^2} \log \frac{M_P^2}{\mu^2}$  and we introduce the notations;

$$\begin{aligned}
Y_{K\eta_8} &= Y_{K\eta} \cos^2 \theta_{08} + Y_{K\eta'} \sin^2 \theta_{08}, \\
\mu_{\eta_8} &= \mu_\eta \cos^2 \theta_{08} + \mu_{\eta'} \sin^2 \theta_{08}.
\end{aligned}$$

$Y_{K\eta_8}$  denotes  $L_{K\eta_8}$ ,  $H_{K\eta_8}^0$  and  $\bar{J}_{K\eta_8}$ .  $l_5^r$  is the finite part of the counterterm of  $L_5$  defined as,

$$L_5 = l_5^r - \frac{3}{256\pi^2} (C_{UV} + 1 - \ln \mu^2). \tag{21}$$

One can make Eq.(19) finite by choosing the counterterms  $C_3$  and  $L_9$ . Because the divergent part of the wavefunction renormalization  $Z_V$  is already determined in Eq.(B6),  $Z_V + \frac{gC_3}{2}$  must be finite. From Eq.(B6) one obtains,

$$C_3 = c_3 + \frac{1}{64\pi^2 g} \left( \frac{M_V^2}{gf^2} \right)^2 (C_{UV} + 1 - \ln \mu^2). \tag{22}$$

$L_9$  can be determined as,

$$L_9 + \frac{C_3}{8g} + \frac{1}{128\pi^2} \left( 1 - \frac{M_V^2}{2g^2f^2} \right) (C_{UV} + 1 - \ln \mu^2) = l_9^r + \frac{c_3}{8g}, \tag{23}$$

where  $l_9^r$  is a finite constant and is related to  $L_9$  as,

$$L_9 = l_9^r - \frac{1}{128\pi^2} \left\{ 1 - \frac{M_V^2}{2g^2 f^2} + \left( \frac{M_V^2}{2g^2 f^2} \right)^2 \right\} (C_{UV} + 1 - \ln \mu^2). \quad (24)$$

Then Eq.(18) becomes,

$$\begin{aligned} \text{Eq.(18)} = & \frac{1}{4\sqrt{2}g^2 f^2} \left[ \left( q_\mu - \frac{\Delta_{K\pi}}{Q^2} Q_\mu \right) \frac{\delta A}{M_V^2 + \delta A} \left\{ \delta A + Q^2 \left( z_V + \frac{gc_3}{2} \right) \right\} \right. \\ & \left. + \frac{\Delta_{K\pi}}{Q^2} Q_\mu \frac{(\delta A + Q^2 \delta B)^2}{M_V^2 + \delta A + Q^2 \delta B} \right] \\ & + \frac{3M_V^2}{8\sqrt{2}g^2 f^2} \left[ \left( q_\mu - \frac{\Delta_{K\pi}}{Q^2} Q_\mu \right) (H_{K\pi}^0 + H_{K\eta_8}^0) - \frac{\Delta_{K\pi} Q_\mu}{Q^2 f^2} (L_{K\pi} + L_{K\eta_8}) \right] \\ & - \frac{1}{2\sqrt{2}} \left\{ f_+(l_9^r + \frac{c_3}{8g}, Q^2) - 1 \right\} \left( q_\mu - \frac{\Delta_{K\pi}}{Q^2} Q_\mu \right) \\ & - \frac{1}{2\sqrt{2}} \frac{\Delta_{K\pi}}{Q^2} Q_\mu \{ f_0(l_9^r, Q^2) - 1 \}, \end{aligned} \quad (25)$$

where  $f_+(l_9, Q^2)$  is given as,

$$f_+(l_9, Q^2) = 1 + \frac{3}{2} \{ H_{K\pi}^0(Q^2) + H_{K\eta_8}^0(Q^2) \} + 2l_9 \frac{Q^2}{f^2}, \quad (26)$$

with,

$$H_{PQ}^0(Q^2) = \frac{1}{f^2} \{ Q^2 M_{PQ}^r(Q^2) - L_{PQ}(Q^2) \}, \quad (27)$$

and it is identical to the vector form factor in chiral perturbation theory [30].

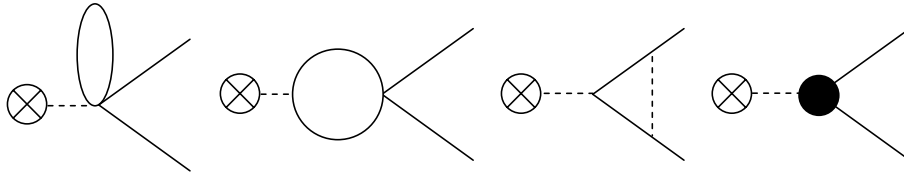


FIG. 2: The one loop Feynman diagrams contributing  $W^+ \rightarrow K^+ \pi^0$  form factors which include one loop corrections to  $K^* \rightarrow K\pi$  vertex. The dashed lines correspond to the vector mesons. The crossed circle denotes the weak vertex. The counterterms contribution to  $K^* \rightarrow K\pi$  vertex are shown as the closed circle. They are given by the terms with their coefficient given by  $C_1, C_2$  and  $C_3$  in Eq.(4).

Next we consider the third category which includes Feynman diagrams corresponding to one loop corrections to  $K^*$  production amplitude as shown in Fig. 3.

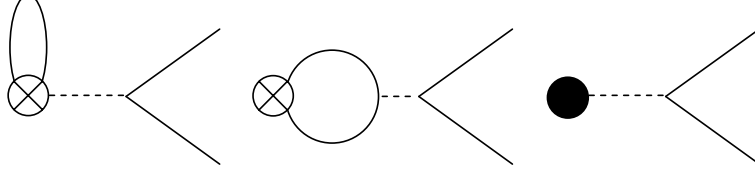


FIG. 3: The one loop Feynman diagrams contributing  $W^+ \rightarrow K^*$  production and subsequent decay into  $K^+\pi^0$ . The dashed lines correspond to the vector mesons. The crossed circle denotes the weak vertex and the closed circle denotes the counterterm respectively.

$$\begin{aligned}
\langle K_\nu^{*+} | \bar{u}_L \gamma_\mu s_L | 0 \rangle &= -\frac{3M_V^2}{8gf^2\sqrt{2}} \left( 1 - \frac{M_V^2}{2g^2f^2} \right) (J_{\mu\nu}^{\pi K} + J_{\mu\nu}^{\eta_8 K}) \\
&+ \frac{1}{\sqrt{2}g} [C_1 m_K^2 + C_2 (2m_K^2 + m_\pi^2)] g_{\mu\nu} + \sqrt{2}C_4 (Q_\mu Q_\nu - Q^2 g_{\mu\nu}) \\
&+ \frac{3M_V^2}{8\sqrt{2}gf^2} (I_\pi + I_{\eta_8} + 2I_K) g_{\mu\nu} \\
&= \frac{1}{\sqrt{2}g} \left[ \left\{ \delta A + Q^2 \delta B - \frac{3M_V^2}{2f^2} (L_{K\pi} + L_{K\eta_8}) \right\} g_{\mu\nu} \right. \\
&\quad \left. + \left\{ z_V - 2gc_4 - \delta B + \frac{3M_V^2}{2f^2} (M_{K\pi}^r + M_{K\eta_8}^r) \right\} (Q^2 g_{\mu\nu} - Q_\mu Q_\nu) \right],
\end{aligned}$$

where we use,

$$Z_V - 2gC_4 = z_V - 2gc_4. \quad (28)$$

With Eq.(30) and Eq.(B6), one obtains,

$$C_4 = c_4 - \frac{1}{256\pi^2 g} \left( \frac{M_V^2}{gf^2} \right)^2 (C_{UV} + 1 - \ln \mu^2). \quad (29)$$

The contribution to the form factor through the process  $W^+ \rightarrow K^{*+} \rightarrow K\pi$  is given as,

$$\begin{aligned}
&\langle K^+\pi^0 | \bar{u}_L \gamma_\mu s_L | 0 \rangle |_{K^{*+}\text{loop}} \\
&= i \frac{q^\rho M_V^2}{4gf^2} \frac{i}{M_V^2 + \delta A} \left( \delta_\rho^\nu - \frac{Q_\rho Q^\nu \delta B}{M_V^2 + \delta A + Q^2 \delta B} \right) \langle K_\nu^{*+} | \bar{u}_L \gamma_\mu s_L | 0 \rangle \\
&= -\frac{M_V^2}{4\sqrt{2}g^2 f^2} \left[ \frac{1}{M_V^2 + \delta A} \left( q_\mu - \frac{\Delta_{K\pi}}{Q^2} Q_\mu \right) \left\{ \delta A + Q^2 (z_V - 2gc_4) + \frac{3M_V^2}{2} (H_{K\pi}^0 + H_{K\eta_8}^0) \right\} \right. \\
&\quad \left. + \frac{1}{M_V^2 + \delta A + Q^2 \delta B} \frac{Q_\mu \Delta_{K\pi}}{Q^2} \left\{ \delta A + Q^2 \delta B - \frac{3M_V^2}{2f^2} (L_{K\pi} + L_{K\eta_8}) \right\} \right]. \quad (30)
\end{aligned}$$

The sum of the amplitudes in the three categories of the diagrams , i.e., Eq.(25) and Eq.(30) is given as,

$$\begin{aligned}
& \text{Eq.(25) + Eq.(30)} \\
&= \frac{\delta A}{4\sqrt{2}g^2f^2} \frac{1}{M_V^2 + \delta A} \left[ \left( q_\mu - \frac{\Delta_{K\pi}}{Q^2} Q_\mu \right) \left\{ Q^2 \left( z_V + \frac{gc_3}{2} \right) + \delta A \right\} \right] \\
&+ \frac{1}{4\sqrt{2}g^2f^2} \frac{\Delta_{K\pi}}{Q^2} Q_\mu \frac{(\delta A + Q^2\delta B)^2}{M_V^2 + \delta A + Q^2\delta B} \\
&+ \frac{3M_V^2}{8\sqrt{2}g^2f^2} \left[ \left( q_\mu - \frac{\Delta_{K\pi}}{Q^2} Q_\mu \right) (H_{K\pi}^0 + H_{K\eta_8}^0) \left( 1 - \frac{M_V^2}{M_V^2 + \delta A} \right) \right. \\
&\left. - \frac{\Delta_{K\pi}}{Q^2} Q_\mu \frac{L_{K\pi} + L_{K\eta_8}}{f^2} \left( 1 - \frac{M_V^2}{M_V^2 + \delta A + Q^2\delta B} \right) \right] \\
&- \frac{1}{2\sqrt{2}} \left[ \left\{ f_+(l_9^r + \frac{c_3}{8g}, Q^2) - 1 \right\} \left( q_\mu - \frac{\Delta_{K\pi}}{Q^2} Q_\mu \right) + \left\{ f_0(l_5^r, Q^2) - 1 \right\} \frac{\Delta_{K\pi}}{Q^2} Q_\mu \right] \\
&- \frac{M_V^2}{4\sqrt{2}g^2f^2} \left[ \frac{1}{M_V^2 + \delta A} \left( q_\mu - \frac{\Delta_{K\pi}}{Q^2} Q_\mu \right) \left\{ \delta A + Q^2(z_V - 2gc_4) \right\} \right] \\
&- \frac{M_V^2}{4\sqrt{2}g^2f^2} \frac{\delta A + Q^2\delta B}{M_V^2 + \delta A + Q^2\delta B} \frac{\Delta_{K\pi} Q_\mu}{Q^2}. \tag{31}
\end{aligned}$$

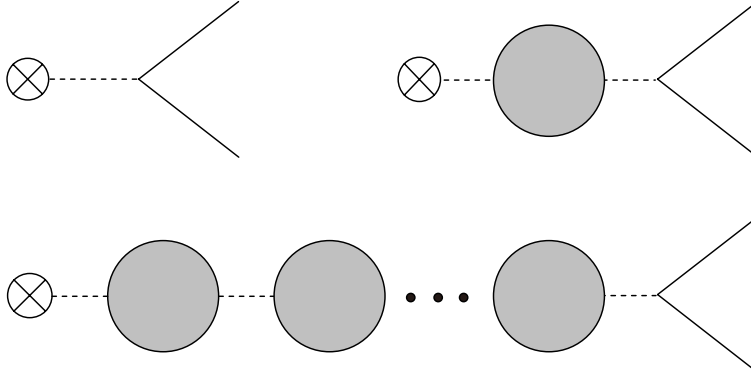


FIG. 4: The contribution to the form factors for  $\tau \rightarrow K\pi\nu$  decay from Dyson sum of the self energy of  $K^*$ . The gray circle denotes the one loop self energy diagrams of  $K^*$ . The crossed circle denotes the weak vertex. The dashed lines are tree level  $K^*$  propagators.

Next we include the contribution from the diagrams of tree level contribution and Dyson sum of the one loop self energy diagram for  $K^*$ . The Feynman diagrams corresponding to them are shown in Fig.4. The infinite numbers of the self energy insertion is equivalent to replacing the tree level propagator with the resummed one in Eq.(16). Using the propagator,

the sum of the tree level contributions is,

$$\begin{aligned}
\langle \pi^0 K^+ | \bar{u}_L \gamma_\mu s_L | 0 \rangle \Big|_{\text{tree+self.}} &= -\frac{1}{2\sqrt{2}} \left( 1 - \frac{M_V^2}{2g^2 f^2} \right) q_\mu - q^\rho D_{\mu\rho} \frac{M_V^4}{4\sqrt{2}g^2 f^2} \\
&= -\frac{1}{2\sqrt{2}} q_\mu + \frac{M_V^2}{4\sqrt{2}g^2 f^2} \left\{ \frac{\delta A}{M_V^2 + \delta A} \left( q_\mu - \frac{\Delta_{K\pi}}{Q^2} Q_\mu \right) \right. \\
&\quad \left. + \frac{\delta A + Q^2 \delta B}{M_V^2 + \delta A + Q^2 \delta B} \frac{Q_\mu \Delta_{K\pi}}{Q^2} \right\}. \tag{32}
\end{aligned}$$

By summing Eq.(32) and Eq.(31), we include all the contributions;

$$\begin{aligned}
\langle K^+ \pi^0 | \bar{u}_L \gamma_\mu s_L | 0 \rangle &= \text{Eq.(32)} + \text{Eq.(31)} \\
&= \frac{\delta A}{4\sqrt{2}g^2 f^2} \frac{1}{M_V^2 + \delta A} \left[ \left( q_\mu - \frac{\Delta_{K\pi}}{Q^2} Q_\mu \right) \left\{ Q^2 (2z_V + \frac{g}{2}(c_3 - 4c_4)) + \delta A \right\} \right] \\
&\quad + \frac{1}{4\sqrt{2}g^2 f^2} \frac{\Delta_{K\pi}}{Q^2} Q_\mu \frac{(\delta A + Q^2 \delta B)^2}{M_V^2 + \delta A + Q^2 \delta B} \\
&\quad + \frac{3M_V^2}{8\sqrt{2}g^2 f^2} \left[ \left( q_\mu - \frac{\Delta_{K\pi}}{Q^2} Q_\mu \right) (H_{K\pi}^0 + H_{K\eta_8}^0) \frac{\delta A}{M_V^2 + \delta A} \right. \\
&\quad \left. - \frac{\Delta_{K\pi}}{Q^2} Q_\mu \frac{L_{K\pi} + L_{K\eta_8}}{f^2} \frac{\delta A + Q^2 \delta B}{M_V^2 + \delta A + Q^2 \delta B} \right] \\
&\quad - \frac{1}{2\sqrt{2}} \left[ f_+(l_{9\text{eff.}}, Q^2) \left( q_\mu - \frac{\Delta_{K\pi}}{Q^2} Q_\mu \right) + f_0(l_5^r, Q^2) \frac{\Delta_{K\pi}}{Q^2} Q_\mu \right], \tag{33}
\end{aligned}$$

where  $l_{9\text{eff.}}$  is given by,

$$l_{9\text{eff.}} = l_9^r + \frac{1}{4g^2} \left\{ z_V + \frac{g}{2}(c_3 - 4c_4) \right\}. \tag{34}$$

Then the vector and scalar form factors can be written as,

$$\begin{aligned}
F_V^{K\pi}(Q^2) &= -\frac{1}{\sqrt{2}} \left[ f_+(l_9', Q^2) - \frac{\delta A}{2g^2 f^2} + \frac{M_V^2}{2g^2 f^2} \frac{\delta A}{M_V^2 + \delta A} \left\{ -\frac{3}{2}(H_{K\pi}^0 + H_{K\eta_8}^0) \right\} \right. \\
&\quad \left. + \frac{M_V^2}{2g^2 f^2} \frac{Q^2}{M_V^2 + \delta A} \left\{ 2z_V + \frac{g}{2}(c_3 - 4c_4) \right\} \right], \tag{35}
\end{aligned}$$

$$\begin{aligned}
F_S^{K\pi}(Q^2) &= -\frac{\Delta_{K\pi}}{Q^2} \frac{1}{\sqrt{2}} \left[ f_0(l_5^r, Q^2) + \frac{M_V^2}{2g^2 f^2} \frac{\delta A + Q^2 \delta B}{M_V^2 + \delta A + Q^2 \delta B} \left( 1 + \frac{3}{2} \frac{L_{K\pi} + L_{K\eta_8}}{f^2} \right) \right. \\
&\quad \left. - \frac{1}{2g^2 f^2} (\delta A + Q^2 \delta B) \right], \tag{36}
\end{aligned}$$

where  $l_9' = l_9^r - \frac{z_V}{4g^2}$ .

#### IV. NUMERICAL ANALYSIS IN THE STANDARD MODEL

To evaluate the vector and scalar form factors, we fix the coefficients of the counterterms by using the decay constants, masses and widths of the mesons. We also use the hadronic

mass spectrum. We set  $f = f_\pi$  and  $\mu = M_{K^*}$ .  $l_5^r$  is fixed with the ratio  $f_K/f_\pi$  [30],

$$\frac{f_K}{f_\pi} = 1 + \frac{1}{4}(5\mu_\pi - 2\mu_K - 3\mu_\eta) + 4\frac{\Delta_{K\pi}}{f_\pi^2}l_5^r. \quad (37)$$

Since  $c_3$  and  $c_4$  are appeared as the set of  $c_3 - 4c_4$  in Eq.(34), there are seven parameters to be determined;  $\{g, M_V, z_V, c_1, c_2, c_3 - 4c_4, l_9^r\}$ . From the imaginary part of the self energy for  $K^*$  meson in Eq.(B8), the decay width of  $K^*$  is given by,

$$\Gamma_{K^*}(M_{K^*}^2) = \frac{1}{16\pi M_{K^*}} \frac{\nu_{K\pi}^3(M_{K^*}^2)}{M_{K^*}^4} \left( \frac{M_V^2}{4gf_\pi^2} \right)^2, \quad (38)$$

where  $\nu_{K\pi}$  is defined in Eq.(B11). Once  $M_V$  is determined,  $g$  can be fixed with the decay width  $K^*$  ( $\Gamma_{K^*}$ ). The relations among  $\mu, z_V, c_1, c_2$  are derived by the conditions for the pole masses of  $K^*$  and  $\rho$  mesons. We define  $K^*$  and  $\rho$  meson masses as the momentum squared ( $Q^2$ ) which corresponds to the values leading the real part of the inverse propagators vanished,

$$M_V^2 + \text{Re}[\delta A_{K^*}(Q^2 = M_{K^*}^2; c_1, c_2)] = 0, \quad (39)$$

$$M_V^2 + \text{Re}[\delta A_\rho(Q^2 = M_\rho^2; c_1, c_2)] = 0. \quad (40)$$

Solving the above equations, one obtains  $c_1$  and  $c_2$ ,

$$c_1 = \frac{1}{\Delta_{K\pi}} \{z_V \Delta_{K^*\rho} - \text{Re}[\Delta A_{K^*}(M_{K^*}^2)] + \text{Re}[\Delta A_\rho(M_\rho^2)]\}, \quad (41)$$

$$c_2 = -\frac{1}{2m_K^2 + m_\pi^2} \{M_V^2 - z_V M_\rho^2 + \text{Re}[\Delta A_\rho(M_\rho^2)] + c_1 m_\pi^2\}, \quad (42)$$

where,

$$\Delta A_{K^*} = -\frac{3}{4} \left( \frac{M_V^2}{gf_\pi^2} \right)^2 \left[ Q^2(M_{K\pi}^r + M_{K\eta_8}^r) - L_{K\pi} - L_{K\eta_8} + \frac{f_\pi^2}{2}(\mu_\pi + 2\mu_K + \mu_{\eta_8}) \right], \quad (43)$$

$$\Delta A_\rho = -\left( \frac{M_V^2}{gf_\pi^2} \right)^2 \left[ Q^2 \left( M_\pi^r + \frac{1}{2}M_K^r \right) + f_\pi^2 \left( \mu_\pi + \frac{1}{2}\mu_K \right) \right]. \quad (44)$$

From the condition for the residue of the vector meson propagator (16),  $z_V$  is written as follows,

$$z_V = 1 + \frac{d\text{Re}[\Delta A_{K^*}(Q^2)]}{dQ^2} \Big|_{Q^2=M_{K^*}^2}. \quad (45)$$

We need to fix the remaining four parameters  $\{g, M_V, c_3 - 4c_4, l_9^r\}$ . Instead of using  $g$  as a fitting parameter, one can use the decay width  $\Gamma_{K^*}$  (See Eq.(38)). Therefore we choose

$\{\Gamma_{K^*}, M_V, c_3 - 4c_4, l'_9\}$  as fitting parameters in the following analysis. We fit them by using the differential branching fraction of the experimental data [22]. The differential branching fraction for  $KP\nu$  ( $P = \pi, \eta$ ) is given by,

$$\begin{aligned} \frac{d\text{Br}(\tau \rightarrow KP\nu)}{d\sqrt{Q^2}} &= \frac{1}{\Gamma_\tau} \frac{G_F^2 |V_{us}|^2 (m_\tau^2 - Q^2)^2}{2^5 \pi^3 m_\tau^3} p_K \\ &\times \left[ \left( \frac{2m_\tau^2}{3Q^2} + \frac{4}{3} \right) p_K^2 |F_V^{KP}(Q^2)|^2 + \frac{m_\tau^2}{2} |F_S^{KP}(Q^2)|^2 \right], \end{aligned} \quad (46)$$

where  $p_K$  is the momentum of  $K$  in the hadronic CM frame. The differential decay distribution for  $\tau^- \rightarrow K_s \pi^- \nu$  is shown in Fig. 5. The  $K^*$  resonance exists in  $\sqrt{Q^2} \simeq 900\text{MeV}$ . We use  $M_{K^*} = 895.53\text{MeV}$  which is obtained in Ref.[22] by treating  $K^*$  resonance contribution as the Breit-Wigner function. The four parameters are determined by fitting the hadronic mass spectrum in the region  $m_K + m_\pi \leq \sqrt{Q^2} \leq 1400.5\text{MeV}$ . The set of parameters leading to the smallest  $\chi^2/\text{n.d.f}$  value are  $\Gamma_{K^*} = 51.0\text{MeV}$ ,  $M_V = 1105.7\text{MeV}$ ,  $c_3 - 4c_4 = 0.26127$ , and  $l'_9 = -2.2555 \times 10^{-4}$ . The obtained  $\chi^2/\text{n.d.f}$  is 109.7/63. We also note  $z_V = 0.81269$  and  $g = 11.042$  for this case. As is seen in Fig. 5, the decay distribution for our prediction (46) is larger than the experimental data in the region  $1400\text{MeV} \lesssim \sqrt{Q^2} \leq m_\tau$ . It is noted that the higher resonances,  $K^*(1410)$  and  $K_0^*(1430)$ , are considered in the study of the experimental data of Ref. [22].

Table I shows the fitted value of  $\Gamma_{K^*}$  and the predictions of the branching fractions of our model. We also show the obtained slope parameter defined in Eq.(48). We use the experimental values,  $m_{\pi^\pm}, f_{\pi^-}, m_{K^0}, m_\eta, m_{\eta'}, m_\tau$  [31] as inputs. In Table I, the branching fraction,  $\text{Br}(\sqrt{Q^2} \leq 1400.5\text{MeV})$  implies the partially integrated branching fraction. We set the upper limit of the integration of the hadronic invariant mass  $\sqrt{Q^2}$  at 1400.5 (MeV).  $\lambda_+$  is the slope parameter given by the linear expansion coefficient of the  $K\pi$  vector form factor (35),

$$F_V^{K\pi}(Q^2) \simeq F_V^{K\pi}(0) \left( 1 + \lambda_+ \frac{Q^2}{m_\pi^2} \right), \quad (47)$$

where,

$$\lambda_+ = \frac{-m_\pi^2}{\sqrt{2}F_V^{K\pi}(0)} \frac{d}{dQ^2} \left[ f_+(l'_9, Q^2) - \frac{\delta A}{2g^2 f^2} - \frac{M_V^2}{2g^2 f^2} \frac{\delta A}{M_V^2 + \delta A} \left\{ \frac{3}{2} (H_{K\pi}^0 + H_{K\eta_8}^0) \right\} \right]_{Q^2=0} \quad (48)$$

To investigate the property of the form factors obtained in the present work, we compare them with the prediction of chiral perturbation. Using the fixed parameters, we show the absolute value and argument for the vector form factors in Figs. 6 and 7. In the

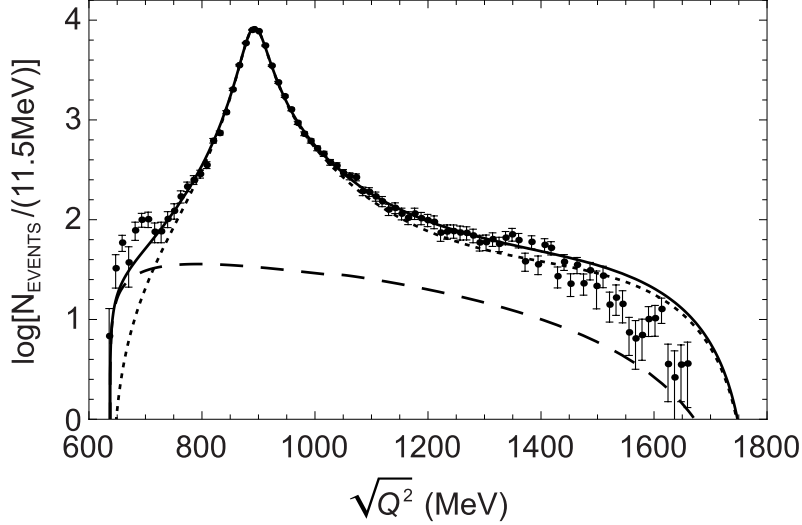


FIG. 5: The prediction of the decay distribution for  $\tau^- \rightarrow K_s \pi^- \nu$ . The solid line corresponds to the prediction of our model. The dotted line and the dashed line correspond to the distribution of the vector form factor and that of the scalar form factor, respectively. The closed circles with the error bars are experimental data [22].

TABLE I: Fitted parameters and obtained values. Last line is the experimental values.

	$\Gamma_{K^*}(\text{MeV})$	$\text{Br}(\sqrt{Q^2} \leq 1400.5 \text{ MeV})$	$\text{Br}(\sqrt{Q^2} \leq m_\tau)$	$\lambda_+$
our model	51.0	0.399%	0.405%	0.0311
experiment	$50.8 \pm 0.9$	0.401%	$(0.404 \pm 0.002 \pm 0.013)\%$	$0.0298 \pm 0.0005$

absolute value of the vector form factor  $|F_V^{K\pi}|$ , the effect of  $K^*$  resonance is dominant at  $\sqrt{Q^2} \simeq M_{K^*}$ . Furthermore, the effect of  $K^*$  resonance is seen in the argument of vector form factor ( $\arg[F_V^{K\pi}]$ ), because it changes about  $180^\circ$  near  $\sqrt{Q^2} \simeq M_{K^*}$ . These properties are also seen in  $K\pi$  scattering [32]. Figures 8 and 9 show the absolute value and argument for the scalar form factors, respectively. The behavior of obtained scalar form factor  $F_S^{K\pi}$  is similar to that of the chiral perturbation result  $f_0$ , because the effect of  $K^*$  resonance in  $F_S^{K\pi}$  is small, e.g., there is no  $K^*$  pole in  $F_S^{K\pi}$  as Eq.(36).

We consider  $\tau^- \rightarrow K^- \eta \nu$  decay using the parameters fixed with  $\tau^- \rightarrow K_s \pi^- \nu$  decay. The equations of the  $K\eta$  form factors are written in Appendix B. Figure 10 shows the prediction of the decay distribution for  $\tau^- \rightarrow K^- \eta \nu$ . It is found that the contribution of vector form factor is dominant. The predicted branching fraction for  $\tau^- \rightarrow K^- \eta \nu$  decay is  $1.60 \times 10^{-4}$ .

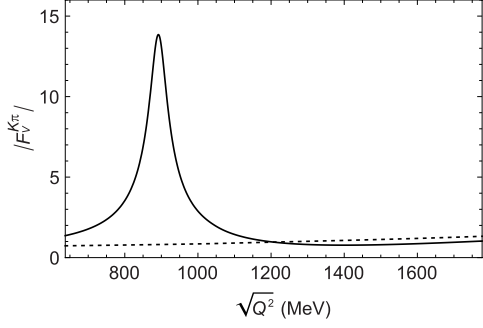


FIG. 6: The absolute values of the vector form factors. The solid line and the dotted line denote  $|F_V^{K^*}|$  and  $|f_{+}|$ , respectively.

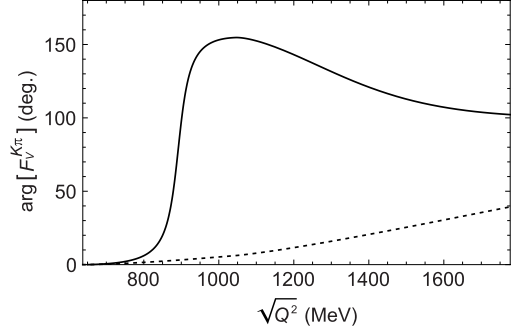


FIG. 7: The arguments of the vector form factors. The solid line and the dotted line denote  $\arg[F_V^{K^*}]$  and  $\arg[f_{+}|$ , respectively.

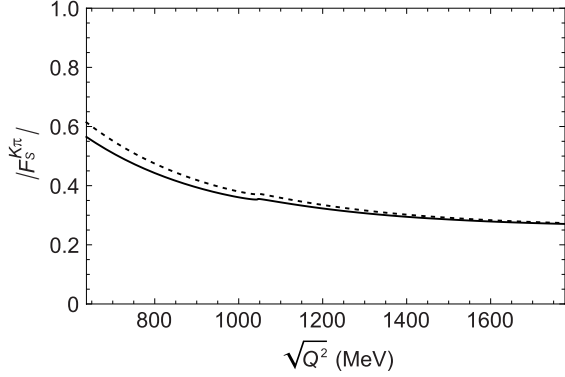


FIG. 8: The absolute values of the scalar form factors. The solid line and the dotted line denote  $|F_S^{K^*}|$  and  $|f_0|$ , respectively.

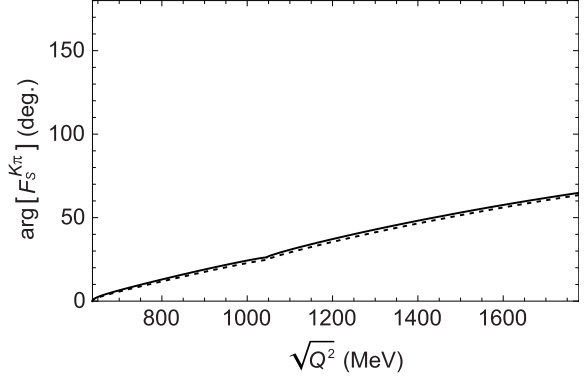


FIG. 9: The arguments of the scalar form factors. The solid line and the dotted line denote  $\arg[F_S^{K^*}]$  and  $\arg[f_0|$ , respectively.

Since the experimental results are  $\text{Br}(\tau^- \rightarrow K^- \eta \nu) = (1.52 \pm 0.08) \times 10^{-4}$  [31], our prediction is slightly larger than the experimental data.

We also consider the forward and backward asymmetry [28] for  $\tau \rightarrow KP\nu$  decay. The double differential rate of the unpolarized  $\tau$  decay [6] is given by

$$\frac{d\text{Br}}{d\sqrt{Q^2}d\cos\theta} = \frac{1}{\Gamma} \frac{G_F^2 |V_{us}|^2 (m_\tau^2 - Q^2)^2 p_K}{2^5 \pi^3 m_\tau^3} \left\{ \left( \frac{m_\tau^2}{Q^2} \cos^2 \theta + \sin^2 \theta \right) p_K^2 |F_V^{KP}(Q^2)|^2 + \frac{m_\tau^2}{4} |F_S^{KP}|^2 - \frac{m_\tau^2}{\sqrt{Q^2}} p_K \cos \theta \text{Re}[F_V^{KP}(Q^2) F_S^{KP}(Q^2)^*] \right\}, \quad (49)$$

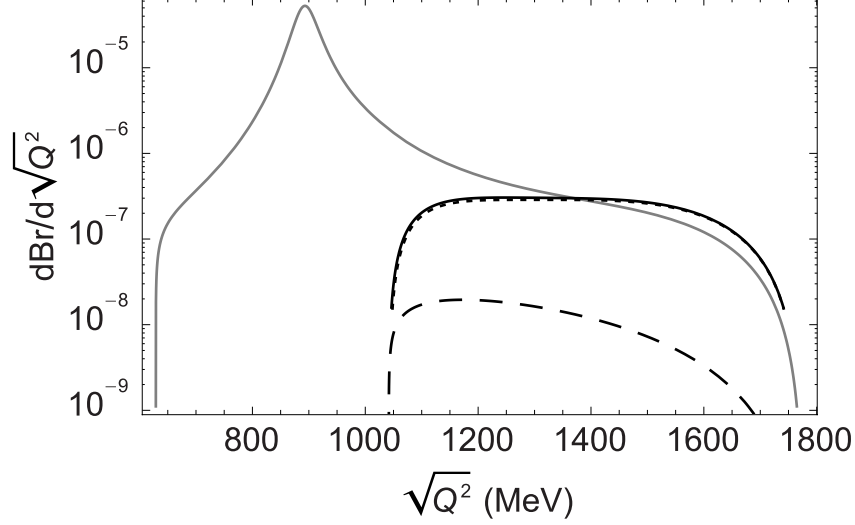


FIG. 10: The hadronic invariant mass distribution for  $\tau^- \rightarrow K^- \eta \nu$  decay. The solid line and the gray solid line correspond to the hadronic invariant mass distribution for  $\tau^- \rightarrow K \eta \nu$  decay and that for  $\tau \rightarrow K_s \pi \nu$  decay, respectively. The dotted line and the dashed line are the vector form factor contribution and the scalar form factor contribution of  $\tau \rightarrow K \eta \nu$  decay, respectively.

where  $\theta$  is the scattering angle of kaon with respect to the incoming  $\tau$  in the hadronic CM frame. The forward and backward asymmetry extracts the interference term of the vector form factor and the scalar form factor.

$$\begin{aligned}
 A_{\text{FB}}(Q^2) &= \frac{\int_0^1 d \cos \theta \frac{d\text{Br}}{d\sqrt{Q^2} d \cos \theta} - \int_{-1}^0 d \cos \theta \frac{d\text{Br}}{d\sqrt{Q^2} d \cos \theta}}{\frac{d\text{Br}}{d\sqrt{Q^2}}} \\
 &= -\frac{\frac{p_K}{\sqrt{Q^2}} \frac{|F_S^{KP}|}{|F_V^{KP}|} \cos \delta_{\text{st}}^{KP}}{\left(\frac{2m^2}{3s} + \frac{4}{3}\right) \frac{p_K^2}{m_\tau^2} + \frac{1}{2} \left|\frac{F_S^{KP}}{F_V^{KP}}\right|^2}, \tag{50}
 \end{aligned}$$

with  $\delta_{\text{st}}^{KP} = \arg\left(\frac{F_V^{KP}}{F_S^{KP}}\right)$ . As we can see from Eq.(50), the forward and the backward asymmetry is determined by the ratio of the scalar and the vector form factors. It is also proportional to cosine of the strong phase shift  $\delta_{\text{st}}^{KP}$ . The forward and backward asymmetries for  $K\pi$  and  $K\eta$  cases are shown in Fig. 11. As can be seen in Fig. 11, the forward and backward asymmetry for  $K\pi$  case is large below  $K^*$  resonance and reaches to 70%. Here the decay distribution for  $\tau^- \rightarrow K_s \pi^- \nu$  is identical to that of  $\tau^- \rightarrow K^- \pi^0 \nu$  by taking the limit for  $\epsilon_K$  of  $K^0 \bar{K}^0$  mixing zero. In Fig. 11, we have evaluated the forward and backward asymmetry for  $\tau^- \rightarrow K^- \pi^0 \nu$  as that for  $K\pi$  case.

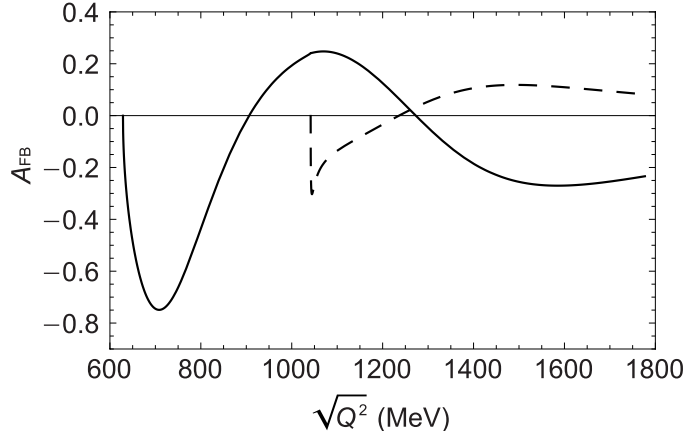


FIG. 11: The predictions of the forward and backward asymmetries of  $\tau \rightarrow K\pi\nu$  and  $\tau \rightarrow K\eta\nu$  decays. The solid line and dashed line correspond to the forward and backward asymmetry of  $\tau \rightarrow K\pi\nu$  decay and that of the  $\tau \rightarrow K\eta\nu$  decay, respectively.

## V. TWO HIGGS DOUBLET MODEL WITH CP VIOLATION

As an example of new physics beyond the standard model, we investigate a two Higgs doublet model [33] with explicit CP violation. The model is classified as type II two-Higgs-doublet model (2HDM).  $Z_2$  parity is assigned so that only a Higgs doublet  $\Phi_2$  is coupled to up type quarks and another Higgs doublet  $\Phi_1$  is coupled with down type quarks. For the charged leptons, they have Yukawa coupling with the same Higgs doublet which the down type quarks interact with.  $Z_2$  symmetry is softly broken in Higgs sector. By taking the soft breaking mass squared parameter small, one can naturally obtain the large ratio of vacuum expectation values (VEVs) of two Higgs doublets. The idea of Ref. [34] is that this large ratio of the Higgs VEVs is the origin of the isospin breaking of the third generation of the quarks. In such model, the Higgs with small VEV has enhanced Yukawa couplings to down type quarks and charged leptons. Therefore,  $\tau$  lepton and bottom quark can be good probes investigating the extra Higgs doublet with the small VEV.

The well known effect of CP violation of the two Higgs doublet model is CP even and CP odd Higgs mixing [35, 36]. In the large limit of the ratio of Higgs VEVs, among three neutral Higgs, the standard model like CP even Higgs is decoupled from the other two Higgs bosons. Therefore, in good approximation, CP even and CP odd Higgs mixing occurs among two Higgs bosons in the sector of the Higgs with the small VEV. We investigate how the

CP violating mixing of the neutral Higgs sector leads to some observable effect on charged Higgs Yukawa coupling. We also explicitly show how it generates the direct CP violation of  $\tau$  decays. For this purpose, we compute one loop corrections to masses of the charged leptons and down type quarks. One finds the one loop corrected mass is flavor diagonal and a small CP violating chiral phase due to the CP even and CP odd Higgs mixing is generated. To remove the phase of one loop corrected mass, one needs to carry out the chiral rotation. After the chiral rotation, CP violating phase in charged Higgs sector arises. The phase is due to the CP violation of Higgs sector which is the different origin from Kobayashi Maskawa phase [37].

After all, the relative CP violating phase difference between the charged current interaction of  $W$  boson and charged Higgs interaction arises as,

$$\mathcal{L} \sim \bar{\nu}_L \gamma_\mu \tau_L W^{\mu+} + \bar{\nu}_L \tau_R H^+ e^{-2i\phi_\tau}. \quad (51)$$

The phase  $\phi_\tau$  vanishes if CP even and CP odd Higgs mixing angle  $\theta_{AH}$  vanishes. The phase  $\phi_\tau$  can be measured by direct CP violation of  $\tau^\pm$  decays. The decays go through the intermediate states  $W^-$  and  $H^-$  which are converted to a common hadronic final state ( $K, \pi$ ). Schematically, the process goes as,

$$\tau \rightarrow \left\{ \begin{array}{l} \nu_L + W^{-*} \\ \nu_L + H^{-*} \end{array} \right\} \rightarrow K^- \pi^0 + \nu. \quad (52)$$

To measure the phase  $\phi_\tau$ , the angular analysis of the decay distributions of  $\tau \rightarrow K\pi\nu$  is useful. The direct CP violation arises in the interference of two amplitudes with both weak phase difference and strong phase difference. In the  $\tau \rightarrow K\pi\nu$  decays, the interference of two amplitudes with different angular momentum of  $K^- \pi^0$ , i.e.,  $l = 1$  and  $l = 0$  can take place. The difference of the angular distribution of  $\tau^- \rightarrow K^- \pi^0 \nu$  and its CP conjugate  $\tau^+ \rightarrow K^+ \pi^0 \bar{\nu}$  is sensitive to the CP violating phase described above. As we have shown in [10], the forward and the backward CP asymmetry is a good observable for the CP violation.

The Higgs potential of two Higgs doublet model with softly broken  $Z_2$  symmetry is given as,

$$\begin{aligned} V_{\text{tree}} = & \sum_{i=1,2} \left( m_i^2 \Phi_i^\dagger \Phi_i + \frac{\lambda_i}{2} (\Phi_i^\dagger \Phi_i)^2 \right) - m_3^2 (\Phi_1^\dagger \Phi_2 + h.c.) + \lambda_3 (\Phi_1^\dagger \Phi_1) (\Phi_2^\dagger \Phi_2) \\ & + \lambda_4 |\Phi_1^\dagger \Phi_2|^2 + \frac{1}{2} \lambda_5 \left[ e^{i\theta_5} (\Phi_2^\dagger \Phi_1)^2 + e^{-i\theta_5} (\Phi_1^\dagger \Phi_2)^2 \right], \end{aligned} \quad (53)$$

where under  $Z_2$  transformation, the Higgs fields transform as,

$$\Phi_1 \rightarrow -\Phi_1, \quad \Phi_2 \rightarrow \Phi_2. \quad (54)$$

$\theta_5$  is a CP violation parameter of Higgs sector. One may write the vacuum expectation values with three order parameters [38],

$$\langle \Phi_1 \rangle = \frac{v}{\sqrt{2}} \begin{pmatrix} 0 \\ \cos \beta \end{pmatrix}, \quad \langle \Phi_2 \rangle = \frac{v}{\sqrt{2}} \begin{pmatrix} 0 \\ \sin \beta \end{pmatrix} e^{-i\theta'}. \quad (55)$$

The three order parameters are determined by the stationary conditions. For large  $\tan \beta$ , the solution can be written approximately as,

$$\begin{aligned} v^2 &\simeq -\frac{2m_2^2}{\lambda_2}, \\ \cos \beta &\simeq \frac{m_3^2}{(m_1^2 + \frac{v^2}{2}(\lambda_3 + \lambda_4)) \cos \theta' + \frac{v^2}{2}\lambda_5 \cos(\theta_5 + \theta')}, \\ \frac{\sin(\theta_5 + \theta')}{\sin \theta'} &\simeq \frac{\lambda_3 + \lambda_4 - \frac{m_1^2}{m_2^2}\lambda_2}{\lambda_5}, \end{aligned} \quad (56)$$

where only the leading terms with respect to the expansion of the soft breaking parameter  $\frac{m_3^2}{m_1^2}$  are shown. When  $\theta_5$  is not vanishing, the neutral Higgs bosons with definite CP parities, i.e., CP even (H) and CP odd Higgs (A) are not mass eigenstates. Their mixing angle is sensitive to the CP violation of the Higgs sector. In large  $\tan \beta$  limit, the mass matrix of the three neutral Higgs becomes,

$$\mathcal{L}_{\text{mass}} = -\frac{v^2}{4}(h, H, A) \begin{pmatrix} a_{11} & 0 & 0 \\ 0 & a_{22} & a_{23} \\ 0 & a_{23} & a_{33} \end{pmatrix} \begin{pmatrix} h \\ H \\ A \end{pmatrix}, \quad (57)$$

where  $a_{12}$  and  $a_{13}$  are subleading of the expansion of  $\cos \beta$  and can be neglected in large  $\tan \beta$  limit. Therefore in the limit, one can simply diagonalize  $2 \times 2$  matrix. For the purpose, one introduces the mixing angle  $\theta_{AH}$ ,

$$\begin{aligned} H &= \cos \theta_{AH} H_3 + \sin \theta_{AH} H_2, \\ A &= \cos \theta_{AH} H_2 - \sin \theta_{AH} H_3, \end{aligned} \quad (58)$$

where  $H_2$  and  $H_3$  are mass eigen states. The other matrix elements in small  $\cos \beta$  limit are,

$$\begin{aligned}
a_{11} &\simeq 2\lambda_2, \\
a_{33} &\simeq \left( \frac{\sin(\theta_5 + \theta')}{\sin \theta'} - \cos(\theta_5 + 2\theta') \right) \lambda_5, \\
a_{22} &\simeq \left( \cos \theta_5 + \cos 2\theta' \frac{\sin(\theta' + \theta_5)}{\sin \theta'} \right) \lambda_5, \\
a_{23} &\simeq -\lambda_5 \sin(\theta_5 + 2\theta').
\end{aligned} \tag{59}$$

Then one finds the mixing angle is given by,

$$\theta_{AH} = \frac{\theta_5}{2} + \theta'. \tag{60}$$

In the same limit, the masses of all the Higgs bosons are;

$$\mathcal{L}_{\text{mass}} = -\frac{M_h^2}{2}h^2 - \frac{M_{H_2}^2}{2}H_2^2 - \frac{M_{H_3}^2}{2}H_3^2 - M_{H^+}^2 H^+ H^-, \tag{61}$$

with,

$$\begin{aligned}
M_h^2 &= \lambda_2 v^2, \\
M_{H^+}^2 &= m_1^2 + \frac{\lambda_3}{2} v^2, \\
M_{H_2}^2 &= m_1^2 + \frac{v^2}{2} (\lambda_3 + \lambda_4 - \lambda_5), \\
M_{H_3}^2 &= m_1^2 + \frac{v^2}{2} (\lambda_3 + \lambda_4 + \lambda_5).
\end{aligned} \tag{62}$$

Using the relations in Eq.(56) and the mass formulae of Higgs bosons in Eq.(62), one can write the formulae  $\cos \beta$  and  $\theta_{AH}$  as follows;

$$\cos \beta = \frac{m_3^2}{\sqrt{M_{H_3}^4 \cos^2 \theta_{AH} + M_{H_2}^4 \sin^2 \theta_{AH}}}, \tag{63}$$

$$\theta_{AH} = \arctan \left[ \frac{M_{H_3}^2}{M_{H_2}^2} \tan \frac{\theta_5}{2} \right]. \tag{64}$$

In Fig.12, we have shown the mixing angle  $\theta_{AH}$  as a function of CP violating parameter  $\theta_5$  of the Higgs potential as given by Eq.(64). One can see when the mass splitting of  $H_2$  and  $H_3$  are large,  $\theta_{AH}$  tends to deviate from the line of  $\theta_{AH} = \frac{\theta_5}{2}$ , which leads to  $\theta'$  is non-vanishing. Next we compute the one loop corrected mass due to  $H_2$  and  $H_3$ . Yukawa couplings of them

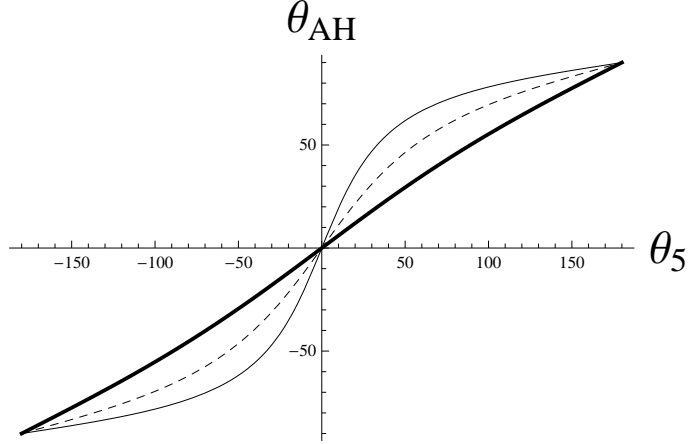


FIG. 12: The CP even and odd Higgs mixing angle  $\theta_{AH}$  as a function of CP violating parameter  $\theta_5$ . The thin solid line, the dashed line, and the thick solid line correspond to  $\frac{M_{H_3}}{M_{H_2}} = 2, 1.5,$  and 1.1, respectively.

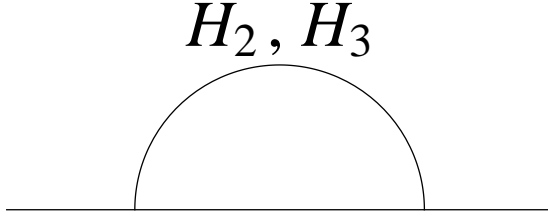


FIG. 13: One loop corrections to the self energies of down type quarks and charged leptons due to neutral Higgs exchanges.

to down type quarks and charged leptons can be written as,

$$\begin{aligned} \mathcal{L}_Y = & \frac{H_2}{v} \left[ \tan \beta (\bar{e}_i i \gamma_5 e^{-i\gamma_5 \theta_{AH}} m_{li} e_i + \bar{d}_i i \gamma_5 e^{-i\gamma_5 \theta_{AH}} m_{di} d_i) \right] \\ & + \frac{H_3}{v} \left[ \tan \beta (\bar{e}_i e^{-i\gamma_5 \theta_{AH}} m_{li} e_i + \bar{d}_i e^{-i\gamma_5 \theta_{AH}} m_{di} d_i) \right]. \end{aligned} \quad (65)$$

Note that the Yukawa couplings of  $H_2$  and  $H_3$  have an enhancement factor  $\tan \beta$ . They are CP violating and the CP violating phase is related to  $\theta_{AH}$ . One defines the one loop corrected masses for down type quarks and charged leptons as,

$$\mathcal{L}_{mass} = -\bar{l}_{Li} M_{li} l_{Ri} - \bar{d}_{Li} M_{di} d_{Ri} + h.c.. \quad (66)$$

The corrections are evaluated by computing Feynman diagrams Fig.13 and the result is,

$$\begin{aligned} M_{l_i} &= m_{l_i} \left( 1 - \left( \frac{m_{l_i} \tan \beta}{4\pi v} \right)^2 \ln \frac{M_{H_2}^2}{M_{H_3}^2} e^{-2i\theta_{AH}} \right), \\ M_{d_i} &= m_{d_i} \left( 1 - \left( \frac{m_{d_i} \tan \beta}{4\pi v} \right)^2 \ln \frac{M_{H_2}^2}{M_{H_3}^2} e^{-2i\theta_{AH}} \right). \end{aligned} \quad (67)$$

In order to remove the phases of the one loop corrected mass, one need to perform the flavor diagonal chiral rotation,

$$\begin{aligned} l_{Ri} &\rightarrow l_{Ri} e^{-i\phi_{l_i}}, & l_{Li} &\rightarrow l_{Li} e^{i\phi_{l_i}}, \\ d_{Ri} &\rightarrow d_{Ri} e^{-i\phi_{d_i}}, & d_{Li} &\rightarrow d_{Li} e^{i\phi_{d_i}}, \end{aligned} \quad (68)$$

where the phases  $\phi_{l_i}$  and  $\phi_{d_i}$  are given by,

$$\tan 2\phi_{l_i} = \frac{\sin 2\theta_{AH} \left( \frac{m_{l_i} \tan \beta}{4\pi v} \right)^2 \ln \frac{M_{H_2}^2}{M_{H_3}^2}}{1 - \left( \frac{m_{l_i} \tan \beta}{4\pi v} \right)^2 \cos 2\theta_{AH} \ln \frac{M_{H_2}^2}{M_{H_3}^2}}, \quad (69)$$

$$\tan 2\phi_{d_i} = \frac{\sin 2\theta_{AH} \left( \frac{m_{d_i} \tan \beta}{4\pi v} \right)^2 \ln \frac{M_{H_2}^2}{M_{H_3}^2}}{1 - \left( \frac{m_{d_i} \tan \beta}{4\pi v} \right)^2 \cos 2\theta_{AH} \ln \frac{M_{H_2}^2}{M_{H_3}^2}}. \quad (70)$$

In Fig.14, we have shown  $\phi_\tau$  for different ratios of the Higgs mass  $\frac{M_{H_3}}{M_{H_2}}$ . The larger ratio leads to the larger value of  $\phi_\tau$ .

Now we study the effects of the CP violation of the Higgs mixing on  $\tau$  lepton decays. The effective four Fermi interactions from the standard model contribution and from the charged Higgs exchange are given by,

$$\begin{aligned} \mathcal{L}_{cc} &= 2\sqrt{2}G_F V_{ji}^* \left[ -\overline{d_{iL}} \gamma_\mu u_{jL} \overline{\nu_L} \gamma^\mu \tau_L \right. \\ &\quad \left. + \frac{m_\tau m_{d_i} \tan^2 \beta}{M_{H^+}^2} \overline{d_{iR}} u_{jL} e^{-2i(\phi_\tau - \phi_{d_i})} \overline{\nu_L} \tau_R \right], \end{aligned} \quad (71)$$

where the relative phase  $\phi_\tau - \phi_{d_i}$  of charged current interaction due to  $W^-$  exchanged and charged Higgs interaction  $H^-$  arises.

The forward and backward CP asymmetry in the two Higgs doublet model can be obtained by replacing the standard model scalar form factor with the one including the charged Higgs contribution in Eq.(50).

$$F_{SNew}^{KP} \equiv \left( 1 - e^{-2i(\phi_\tau - \phi_s)} \frac{Q^2 \tan^2 \beta}{M_{H^+}^2} \right) F_S^{KP} \quad (72)$$

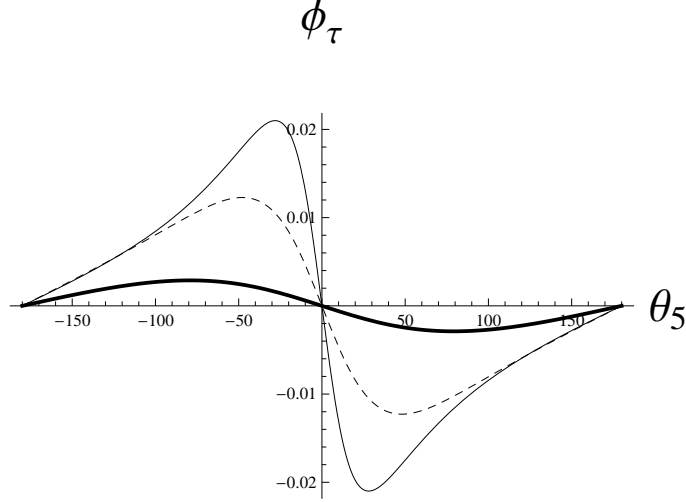


FIG. 14:  $\phi_\tau$  as a function of  $\theta_5$ . The unit of the angles is in degree. The thin solid line, the dashed line, and the thick solid line correspond to  $\frac{M_{H_3}}{M_{H_2}} = 2, 1.5,$  and  $1.1,$  respectively.

By comparing the forward and backward asymmetry of  $\tau^-$  and  $\tau^+$ , one obtains the direct CP violation [10],

$$\begin{aligned}
& A_{FB}(\tau^- \rightarrow K^- \pi^0 \nu) - \overline{A}_{FB}(\tau^+ \rightarrow K^+ \pi^0 \overline{\nu}) \\
&= -2 \sin \delta_{st}^{KP} \sin\{2(\phi_\tau - \phi_s)\} \frac{Q^2 \tan^2 \beta}{M_{H^+}^2} \frac{\frac{p_K}{\sqrt{Q^2}} \frac{|F_S^{KP}|}{|F_V^{KP}|}}{\left(\frac{2m_\tau^2}{3Q^2} + \frac{4}{3}\right) \frac{p_K^2}{m_\tau^2} + \frac{1}{2} \frac{|F_{SNeu}^{KP}|^2}{|F_V^{KP}|^2}}, \quad (73)
\end{aligned}$$

To predict the CP violation, we take account of the constraints on the mass of the charged Higgs,  $\tan \beta$  and the ratio of neutral Higgs masses  $\frac{M_{H_3}}{M_{H_2}}$ . The lower limit of the charged Higgs mass is given as  $M_{H^+} > 300$  (GeV) obtained from  $b \rightarrow s\gamma$ . Using  $B \rightarrow \tau\nu$  and  $B \rightarrow D\tau\nu$ , the lower limit of the charged Higgs mass is constrained as  $M_{H^+} > 500$  (GeV) for  $\tan \beta \simeq 40$  [39]. The ratio  $\frac{M_{H_3}}{M_{H_2}}$  of the neutral Higgs masses can be constrained from  $T$  parameter.  $T$  parameter of the present model is computed as,

$$T_{\text{New}} = \frac{1}{16\pi M_W^2 s_W^2} \left( F(M_{H^+}, M_{H_3}) + F(M_{H^+}, M_{H_2}) - F(M_{H_3}, M_{H_2}) \right), \quad (74)$$

where  $F(m_a, m_b)$  is given by,

$$F(m_a, m_b) = \frac{m_a^2 + m_b^2}{2} - \frac{m_a^2 m_b^2 \log \frac{m_a^2}{m_b^2}}{m_a^2 - m_b^2}. \quad (75)$$

The experimental constraint on  $T_{\text{New}}$  is given as [31],

$$T_{\text{New}} = 0.04 \pm 0.11, \quad (76)$$

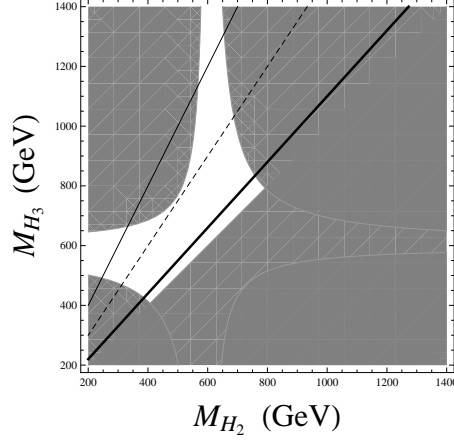


FIG. 15: The constraints on  $T$  parameter in  $(M_{H_2}, M_{H_3})$  plane. The gray shaded regions are excluded. We choose  $M_{H^+} = 600(\text{GeV})$ . The upper bound on  $T_{\text{New}}$  is 0.15 and the lower bound is  $-0.068$ , respectively. The thick solid line, the dashed line, and the thin solid line correspond to  $\frac{M_{H_3}}{M_{H_2}} = 1.1, 1.5$ , and  $2$ , respectively.

for the standard model like Higgs mass  $M_h$  is 126 (GeV) [40]. With  $M_{H^+} = 600$  (GeV), the constraints on  $(M_{H_2}, M_{H_3})$  plane are shown in Fig. 15.

In Fig. 16, the forward and backward CP asymmetry in Eq.(73) is shown. We neglect  $\phi_s$  in the numerical calculation. We choose the charged Higgs mass  $M_{H^+} = 600$  (GeV) and  $\tan \beta = 40$ , and  $\frac{M_{H_3}}{M_{H_2}} = 1.1, 1.5$ , and  $2$  which satisfy the constraints studied. The CP asymmetry is as small as  $10^{-6}$ . Comparing the present result with the one with the two Higgs doublet model without natural flavor conservation [10], the asymmetry is much smaller in the present model because it is the one-loop effect.

## VI. SUMMARY AND CONCLUSION

Now we summarize our results. About the form factors calculation, we apply the chiral Lagrangian including the vector resonance for the computation of the scalar and vector form factors of  $\tau \rightarrow K\pi(\eta)\nu$  decays.

- We determine the new counter terms related to the vector mesons of the Lagrangian.
- By using the method of resummation of the self-energy diagrams of the vector mesons, one can reproduce the vector meson intermediate states.

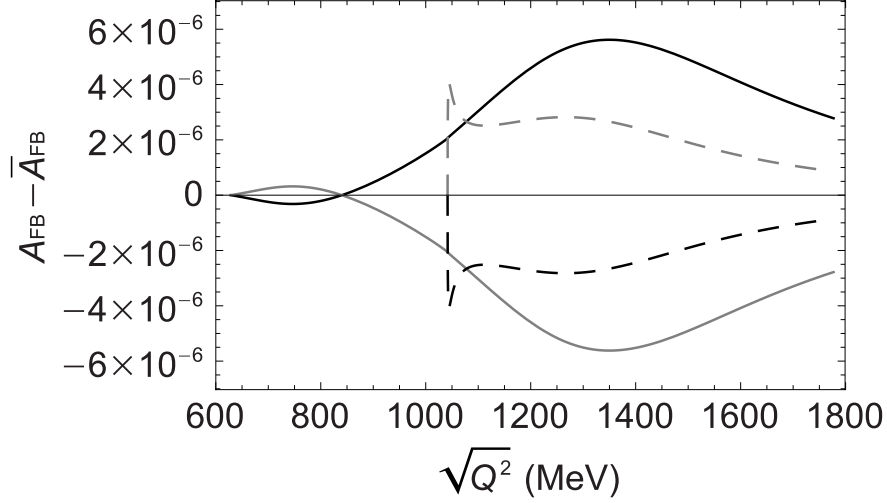


FIG. 16: Forward and backward CP asymmetry  $A_{FB} - \bar{A}_{FB}$  as a function of hadronic invariant mass  $\sqrt{Q^2}$ . The solid lines correspond to the ones of  $\tau \rightarrow K\pi\nu$  decay and the long dashed lines correspond to the ones of  $\tau \rightarrow K\eta\nu$  decay. The gray lines correspond to  $\phi_\tau = 0.02^\circ$  and the black lines correspond to  $\phi_\tau = -0.02^\circ$ . We choose the ratio of the neutral Higgs mass as  $\frac{M_{H_3}}{M_{H_2}} = 2$ , and assume the charged Higgs mass as  $M_{H^+} = 600(\text{GeV})$ .

- We fit our theoretical curve of the hadronic invariant mass distribution with that obtained by Belle. By tuning the parameters, we demonstrate that one can fit the hadronic mass distribution up to  $\sim 1400(\text{MeV})$  well. Above  $1400(\text{MeV})$  and below  $m_\tau \sim 1780(\text{MeV})$ , our prediction exceeds over the experimental result. We also compute the branching fraction  $\tau \rightarrow K\eta\nu$ , which is consistent with the experimental one within  $1\sigma$ .

About the CP violation of the two Higgs doublet model, we study the CP violation of the Higgs sector. The model was invented to explain the large isospin breaking of bottom and top due to large  $\tan\beta \simeq 40$  [34]. CP violation of Higgs potential leads to the mixings of CP even and CP odd Higgs. The Yukawa couplings of down quarks and charged leptons with the neutral Higgs of the second Higgs doublet are large and are CP violating. We found that;

- The CP violation in the neutral Higgs sector leads to the CP violating effect on the quarks and leptons mass matrices through one loop corrections.

- After removing the CP violating phases in the mass matrices, one obtains CP violating phases of the charged Higgs couplings to the down quarks and charged leptons.
- The effect is studied in the forward and backward CP asymmetry of  $\tau \rightarrow K\pi\nu$  decay. The order of the asymmetry is  $10^{-6}$ . The smallness of the asymmetry comes from the fact that the CP violation is 1 loop induced effect.

## Acknowledgments

We would like to thank Dr. D. Epifanov for providing us with the data of Belle. We would like to thank Dr. H. Takata for providing us with the mathematica program of the two Higgs doublet model. We also thank K. Nakagawa, prof. H. Hayashii, Dr. M. Bischofberger and the members of the physics study group of the B factory for fruitful discussion. K.Y.L. was supported by WCU program through the KOSEF funded by the MEST (R31-2008-000-10057-0) and the Basic Science Research Program through the NRF funded by MEST (2010-0010916). The work of T. M. is supported by KAKENHI, Grant-in-Aid for Scientific Research(C) No.22540283 from JSPS, Japan.

## Appendix A: 1 loop functions

Here we summarize the one loop functions which appear in Eq.(13).

$$\begin{aligned}
I_P &= - \int \frac{d^d k}{(2\pi)^{d_i}} \frac{1}{k^2 - m_P^2}, \\
\chi_\mu^{QP} &= \int \frac{d^d k}{(2\pi)^{d_i}} \frac{(Q - 2k)_\mu}{\{(k - Q)^2 - m_Q^2\}(k^2 - m_P^2)}, \\
J_\mu^{QP} &= \int \frac{d^d k}{(2\pi)^{d_i}} \frac{(2k - Q)_\mu (2k - Q)_\nu q^\nu}{\{(k - Q)^2 - m_Q^2\}(k^2 - m_P^2)}, \\
I_\mu^{QP} &= \int \frac{d^d k}{(2\pi)^{d_i}} \frac{(k + 2p_\pi) \cdot (k - 2p_K)(2k - q)_\mu}{\{(k + p_\pi)^2 - m_P^2\}\{(k - p_K)^2 - m_Q^2\}}. \tag{A1}
\end{aligned}$$

By taking account of  $\eta_0$  and  $\eta_8$  mixing, one defines  $I_{\eta_8}$  and  $X_\mu^{\eta_8 K}$  ( $X_\mu = \chi_\mu, J_\mu, I_\mu$ ) as,

$$\begin{aligned}
I_{\eta_8} &= I_\eta \cos^2 \theta_{08} + I_{\eta'} \sin^2 \theta_{08}, \\
X_\mu^{\eta_8 K} &= X_\mu^{\eta K} \cos^2 \theta_{08} + X_\mu^{\eta' K} \sin^2 \theta_{08}. \tag{A2}
\end{aligned}$$

## Appendix B: Two point function of vector mesons

Let us determine the coefficient of the counterterms  $C_1, C_2$  and  $Z_V$  from the renormalization for self-energy of vector mesons. The vector mesons couplings with pseudo scalar mesons in  $\mathcal{L}$  are,

$$\begin{aligned}\mathcal{L}^{VPP} &= -\frac{M_V^2}{gf^2i} \text{Tr}(V_\mu[\pi, \partial^\mu \pi]) \\ &= \frac{M_V^2 i}{4gf^2} \left[ K^{*\mu} \left( K^- \overleftrightarrow{\partial}_\mu \pi^0 + \sqrt{3} K^- \overleftrightarrow{\partial}_\mu \eta_8 + \sqrt{2} \bar{K}^0 \overleftrightarrow{\partial} \pi^- \right) \right. \\ &\quad \left. + 2\rho^{+\mu} \left( \pi^- \overleftrightarrow{\partial} \pi^0 + \frac{1}{\sqrt{2}} \bar{K}^0 \overleftrightarrow{\partial} K^- \right) \right].\end{aligned}\tag{B1}$$

One can parameterize the inverse propagators of vector fields as,

$$A_V g^{\mu\nu} + B_V Q^\mu Q^\nu.\tag{B2}$$

We study the two point functions for  $\rho^+$  and  $K^{*+}$  mesons.

$$\begin{aligned}A_V &= M_V^2 - Q^2 + \delta A_V, \\ B_V &= 1 + \delta B_V,\end{aligned}\tag{B3}$$

where  $\delta A_V$  and  $\delta B_V$  denote the one loop corrections including the contribution from the counterterms. For the  $\rho$  meson, they are given as,

$$\begin{aligned}\delta B_\rho &= z_V(\mu) + \left( \frac{M_V^2}{gf^2} \right)^2 \left( M_\pi^r + \frac{1}{2} M_K^r \right), \\ \delta A_\rho &= -Q^2 \delta B_\rho - \left( \frac{M_V^2}{gf^2} \right)^2 \left( \mu_\pi + \frac{1}{2} \mu_K \right) f^2 \\ &\quad + c_1(\mu) m_\pi^2 + c_2(\mu) (2m_K^2 + m_\pi^2),\end{aligned}\tag{B4}$$

where  $\mu_P = \frac{M_P^2}{32\pi^2 f^2} \ln \frac{M_P^2}{\mu^2}$ .  $M_P^r$  ( $P = \pi, K$ ) are the loop functions for  $\pi$  mesons and  $K$  mesons defined as,

$$\begin{aligned}M_P^r &= \frac{1}{12} \left[ \left( 1 - \frac{4M_P^2}{Q^2} \right) \bar{J}_P - \frac{1}{16\pi^2} \ln \frac{M_P^2}{\mu^2} - \frac{1}{48\pi^2} \right], \\ \bar{J}_P &= \begin{cases} -\frac{1}{16\pi^2} \sqrt{1 - \frac{4M_P^2}{Q^2}} \ln \frac{1 + \sqrt{1 - \frac{4M_P^2}{Q^2}}}{1 - \sqrt{1 - \frac{4M_P^2}{Q^2}}} + \frac{1}{8\pi^2} + i \frac{1}{16\pi} \sqrt{1 - \frac{4M_P^2}{Q^2}}, & (Q^2 \geq 4M_P^2), \\ \frac{1}{8\pi^2} \left( 1 - \sqrt{\frac{4M_P^2}{Q^2} - 1} \arctan \frac{1}{\sqrt{\frac{4M_P^2}{Q^2} - 1}} \right), & (Q^2 \leq 4M_P^2). \end{cases}\end{aligned}\tag{B5}$$

$z_V(\mu)$ ,  $c_1(\mu)$  and  $c_2(\mu)$  are finite parts of the renormalization constants defined by,

$$\begin{aligned} Z_V &= z_V(\mu) - \frac{1}{128\pi^2} \left( \frac{M_V^2}{gf^2} \right)^2 (C_{UV} + 1 - \ln \mu^2), \\ C_1 &= c_1(\mu) - \frac{3}{128\pi^2} \left( \frac{M_V^2}{gf^2} \right)^2 (C_{UV} + 1 - \ln \mu^2), \\ C_2 &= c_2(\mu) - \frac{1}{128\pi^2} \left( \frac{M_V^2}{gf^2} \right)^2 (C_{UV} + 1 - \ln \mu^2), \end{aligned} \quad (\text{B6})$$

with  $C_{UV}$  is the divergent part of the dimensional regularization,

$$C_{UV} = \frac{1}{\epsilon} - \gamma + \ln(4\pi), \quad (\text{B7})$$

where  $\epsilon = 2 - \frac{d}{2}$  and  $\gamma$  is Euler constant. The self energy corrections to  $K^*$  meson are given as,

$$\begin{aligned} \delta B_{K^*} &= z_V(\mu) + \frac{3}{4} \left( \frac{M_V^2}{gf^2} \right)^2 (M_{K\pi}^r + M_{K\eta_8}^r), \\ \delta A_K^* &= -Q^2 \delta B_{K^*} + \frac{3}{4} \left( \frac{M_V^2}{gf^2} \right)^2 \left[ L_{K\pi} + L_{K\eta_8} - \frac{f^2}{2} (\mu_\pi + 2\mu_K + \mu_{\eta_8}) \right] \\ &\quad + c_1(\mu) m_K^2 + c_2(\mu) (2m_K^2 + m_\pi^2), \end{aligned} \quad (\text{B8})$$

where  $M_{PQ}^r$  and  $L_{PQ}$  are the same functions as the ones defined in Gasser Leutwyler,

$$\begin{aligned} M_{PQ}^r &= \frac{1}{12Q^2} (Q^2 - 2\Sigma_{PQ}) \bar{J}_{PQ} + \frac{\Delta_{PQ}^2}{3Q^4} \left[ \bar{J}_{PQ} - Q^2 \frac{1}{32\pi^2} \left( \frac{\Sigma_{PQ}}{\Delta_{PQ}^2} + 2 \frac{M_P^2 M_Q^2}{\Delta_{PQ}^3} \ln \frac{M_Q^2}{M_P^2} \right) \right] \\ &\quad - \frac{k_{PQ}}{6} + \frac{1}{288\pi^2}, \\ L_{PQ} &= \frac{\Delta_{PQ}^2}{4s} \bar{J}_{PQ}, \end{aligned} \quad (\text{B9})$$

where  $k_{PQ} = \frac{(\mu_P - \mu_Q)f^2}{\Delta_{PQ}}$ .  $J_{PQ}$  is a one loop scalar function of pseudo scalar mesons with masses  $M_P$  and  $M_Q$ , Above the threshold;  $Q^2 \geq (M_P + M_Q)^2$ , it is given by,

$$\begin{aligned} \bar{J}_{PQ}(Q^2) &= \frac{1}{32\pi^2} \left[ 2 + \frac{\Delta_{PQ}}{Q^2} \ln \frac{M_Q^2}{M_P^2} - \frac{\Sigma_{PQ}}{\Delta_{PQ}} \ln \frac{M_Q^2}{M_P^2} \right. \\ &\quad \left. - \frac{\nu_{PQ}}{Q^2} \ln \frac{(Q^2 + \nu_{PQ})^2 - \Delta_{PQ}^2}{(Q^2 - \nu_{PQ})^2 - \Delta_{PQ}^2} \right] + \frac{i}{16\pi} \frac{\nu_{PQ}}{Q^2}, \end{aligned} \quad (\text{B10})$$

where,

$$\nu_{PQ}^2 = Q^4 - 2Q^2 \Sigma_{PQ} + \Delta_{PQ}^2, \quad (\text{B11})$$

while below the threshold  $(M_P - M_Q)^2 \leq Q^2 \leq (M_P + M_Q)^2$ ,

$$\bar{J}_{PQ}(Q^2) = \frac{1}{32\pi^2} \left[ 2 + \frac{\Delta_{PQ}}{Q^2} \ln \frac{M_Q^2}{M_P^2} - \frac{\Sigma_{PQ}}{\Delta_{PQ}} \ln \frac{M_Q^2}{M_P^2} - 2 \frac{\sqrt{-\nu_{PQ}^2}}{Q^2} \left( \arctan \frac{Q^2 - \Delta_{PQ}}{\sqrt{-\nu_{PQ}^2}} + \arctan \frac{Q^2 + \Delta_{PQ}}{\sqrt{-\nu_{PQ}^2}} \right) \right], \quad (\text{B12})$$

with  $\Sigma = M_P^2 + M_Q^2$  and  $\Delta_{PQ} = M_P^2 - M_Q^2$ .

### Appendix C: The form factors for $\tau \rightarrow K\eta\nu$ decay and $\tau \rightarrow K\eta'\nu$ decay

In this appendix, we give the equations of the form factors for  $\tau \rightarrow K\eta\nu$  and  $\tau \rightarrow K\eta'\nu$ . In the following equations,  $\delta A$  and  $\delta B$  imply  $\delta A_{K^*}$  and  $\delta B_{K^*}$ , respectively.

$$\begin{aligned} F_V^{K\eta} &= -\frac{\sqrt{3} \cos \theta_{08}}{\sqrt{2}} \left[ f_+(l'_9, Q^2) - \frac{\delta A}{2g^2 f^2} + \frac{M_V^2}{2g^2 f^2} \frac{\delta A}{M_V^2 + \delta A} \left\{ 1 - \frac{3}{2} (H_{K\pi}^0 + H_{K\eta_8}^0) \right\} \right. \\ &\quad \left. + \frac{M_V^2}{2g^2 f^2} \frac{Q^2}{M_V^2 + \delta A} \left\{ 2z_V + \frac{g}{2} (c_3 - 4c_4) \right\} \right], \\ F_S^{K\eta} &= -\frac{\Delta_{K\eta} \cos \theta_{08}}{Q^2} \frac{\sqrt{3}}{\sqrt{2}} \left[ f_0^{K\bar{\eta}}(l'_5, Q^2) + \frac{M_V^2}{2g^2 f^2} \frac{\delta A + Q^2 \delta B}{M_V^2 + \delta A + Q^2 \delta B} \left( 1 + \frac{3}{2} \frac{L_{K\pi} + L_{K\eta_8}}{f^2} \right) \right. \\ &\quad \left. - \frac{1}{2g^2 f^2} (\delta A + Q^2 \delta B) \right], \end{aligned} \quad (\text{C1})$$

$$\begin{aligned} F_V^{K\eta'} &= -\frac{\sqrt{3} \sin \theta_{08}}{\sqrt{2}} \left[ f_+(l'_9, Q^2) - \frac{\delta A}{2g^2 f^2} + \frac{M_V^2}{2g^2 f^2} \frac{\delta A}{M_V^2 + \delta A} \left\{ 1 - \frac{3}{2} (H_{K\pi}^0 + H_{K\eta_8}^0) \right\} \right. \\ &\quad \left. + \frac{M_V^2}{2g^2 f^2} \frac{Q^2}{M_V^2 + \delta A} \left\{ 2z_V + \frac{g}{2} (c_3 - 4c_4) \right\} \right], \\ F_S^{K\eta'} &= -\frac{\Delta_{K\eta} \sin \theta_{08}}{Q^2} \frac{\sqrt{3}}{\sqrt{2}} \left[ f_0^{K\bar{\eta}}(l'_5, Q^2) + \frac{M_V^2}{2g^2 f^2} \frac{\delta A + Q^2 \delta B}{M_V^2 + \delta A + Q^2 \delta B} \left( 1 + \frac{3}{2} \frac{L_{K\pi} + L_{K\eta_8}}{f^2} \right) \right. \\ &\quad \left. - \frac{1}{2g^2 f^2} (\delta A + Q^2 \delta B) \right], \end{aligned} \quad (\text{C2})$$

where

$$\begin{aligned} f_0^{K\bar{\eta}}(l'_5, Q^2) &= 1 + \frac{3}{8f^2} \left( 3Q^2 - 2\Sigma_{K\pi} - \frac{\Delta_{K\pi}^2}{Q^2} \right) \bar{J}_{K\pi}(Q^2) \\ &\quad + \frac{1}{24f^2} \left( -9Q^2 + 2m_K^2 - \frac{\Delta_{K\pi}^2}{Q^2} \right) \bar{J}_{K\eta_8}(Q^2) \\ &\quad + \frac{3}{4f^2} \left\{ m_\eta^2 \bar{J}_{K\eta}(Q^2) \cos^2 \theta_{08} + m_{\eta'}^2 \bar{J}_{K\eta'}(Q^2) \sin^2 \theta_{08} \right\} \\ &\quad + \frac{9Q^2}{4\Delta_{K\pi}} (\mu_\pi - 2\mu_K + \mu_{\eta_8}) + 4 \frac{l'_5}{f^2} Q^2. \end{aligned} \quad (\text{C3})$$

- 
- [1] C. A. Nelson, H. S. Friedman, S. Goozovat, J. A. Klein, L. R. Kneller, W. J. Perry, S. A. Ustin, Phys. Rev. **D50**, 4544 (1994).
- [2] U. Kilian, J. G. Korner, K. Schilcher, Y. L. Wu, Z. Phys. **C62**, 413 (1994).
- [3] Y. S. Tsai, Phys. Rev. **D51**, 3172 (1995).
- [4] S. Y. Choi, K. Hagiwara, M. Tanabashi, Phys. Rev. **D52**, 1614 (1995).
- [5] M. Finkemeier and E. Mirkes, Z. Phys. C **72**, 619 (1996).
- [6] J. H. Kuhn and E. Mirkes, Phys. Lett. B **398**, 407 (1997).
- [7] S. Y. Choi, J. Lee, J. Song, Phys. Lett. **B437**, 191 (1998).
- [8] A. Datta, K. Kiers, D. London, P. J. O'Donnell, A. Szynekman, Phys. Rev. **D75**, 074007 (2007).
- [9] K. Kiers, K. Little, A. Datta, D. London, M. Nagashima and A. Szynekman, Phys. Rev. D **78**, 113008 (2008).
- [10] D. Kimura, K. Y. Lee, T. Morozumi, K. Nakagawa, Nucl. Phys. Proc. Suppl. **189**, 84 (2009).
- [11] D. Kimura, K. Y. Lee, T. Morozumi and K. Nakagawa, Nucl. Phys. Proc. Suppl. **218**, 3 (2011).
- [12] G. Lopez Castro, L. Lopez-Lozano, A. Rosado, Phys. Rev. **D80**, 096004 (2009).
- [13] P. Avery *et al.* [CLEO Collaboration], Phys. Rev. **D64**, 092005 (2001).
- [14] G. Bonvicini *et al.* [CLEO Collaboration], Phys. Rev. Lett. **88**, 111803 (2002).
- [15] M. Bischofberger *et al.* [The Belle Collaboration], Phys. Rev. Lett. **107**, 131801 (2011).
- [16] K. Inami *et al.* [Belle Collaboration], Phys. Lett. B **551**, 16 (2003).
- [17] S. Fajfer, J. Zupan, Int. J. Mod. Phys. **A14**, 4161 (1999).
- [18] M. Jamin, A. Pich and J. Portoles, Phys. Lett. B **640**, 176 (2006); B **664**, 78 (2008).
- [19] B. Moussallam, Eur. Phys. J. **C53**, 401 (2008).
- [20] D. R. Boito, R. Escribano and M. Jamin, Eur. Phys. J. C **59**, 821 (2009).
- [21] V. Bernard, M. Oertel, E. Passemar, J. Stern, Phys. Rev. **D80**, 034034 (2009).
- [22] D. Epifanov *et al.* [ Belle Collaboration ], Phys. Lett. **B654**, 65-73 (2007).
- [23] M. Bando, T. Kugo, S. Uehara, K. Yamawaki, T. Yanagida, Phys. Rev. Lett. **54**, 1215 (1985).
- [24] M. Harada and K. Yamawaki, Phys. Rept. **381**, 1 (2003).
- [25] B. Aubert *et al.* [ BABAR Collaboration ], Phys. Rev. **D76**, 051104 (2007).

- [26] K. Inami *et al.* [ Belle Collaboration ], Phys. Lett. **B672**, 209 (2009).
- [27] P. del Amo Sanchez *et al.* [ The BaBar Collaboration ], Phys. Rev. **D83**, 032002 (2011).
- [28] L. Beldjoudi and T. N. Truong, Phys. Lett. B **351**, 357 (1995).
- [29] J. Gasser, H. Leutwyler, Nucl. Phys. **B250**, 465 (1985).
- [30] J. Gasser, H. Leutwyler, Nucl. Phys. **B250**, 517 (1985).
- [31] K. Nakamura *et al.* [ Particle Data Group Collaboration ], J. Phys. G **G37**, 075021 (2010).
- [32] D. Aston *et al.* Nucl. Phys. B **296**, 493 (1988).
- [33] G. C. Branco, P. M. Ferreira, L. Lavoura, M. N. Rebelo, M. Sher and J. P. Silva, arXiv:1106.0034 [hep-ph].
- [34] M. Hashimoto and S. Kanemura, Phys. Rev. D **70**, 055006 (2004), Erratum-ibid. D **70**, 119901 (2004).
- [35] E. Asakawa, J. i. Kamoshita, A. Sugamoto and I. Watanabe, Eur. Phys. J. C **14**, 335 (2000).
- [36] A. Pilaftsis and C. E. M. Wagner, Nucl. Phys. B **553**, 3 (1999).
- [37] M. Kobayashi and T. Maskawa, Prog. Theor. Phys. **49**, 652 (1973).
- [38] T. Morozumi, H. Takata and K. Tamai, arXiv:1107.1026 [hep-ph].
- [39] M. Bona *et al.* [UTfit Collaboration], Phys. Lett. B **687**, 61 (2010).
- [40] [Atlas collaboration], Atlas note, Atlas-Conf-2011-163, (2011).